catalysts

MDPI

Article

Pyridine-Chelated Imidazo[1,5-*a*]Pyridine *N*-Heterocyclic Carbene Nickel(II) Complexes for Acrylate Synthesis from Ethylene and CO_2

Jiyun Kim [1], Hyungwoo Hahm [1], Ji Yeon Ryu [2], Seunghwan Byun [1], Da-Ae Park [1], Seoung Ho Lee [3], Hyunseob Lim [1], Junseong Lee [2] and Sukwon Hong [1,4,*]

1 Department of Chemistry, Gwangju Institute of Science and Technology, 123 Cheomdan-gwagiro, Buk-gu, Gwangju 61005, Korea; kjiyun@gist.ac.kr (J.K.); hyungwoo@gist.ac.kr (H.H.); sbyun1001@gist.ac.kr (S.B.); daae@gist.ac.kr (D.-A.P.); hslim17@gist.ac.kr (H.L.)
2 Department of Chemistry, Chonnam National University, 77 Yongbongro, Buk-gu, Gwangju 61186, Korea; jy5330@naver.com (J.Y.R.); leespy@chonnam.ac.kr (J.L.)
3 Department of Chemistry, Institute of Basic Sciences, Daegu University, 201 Daegudae-ro, Jillyang-eup, Gyeongsan-si, Gyeongsangbuk-do 38453, Korea; slee@daegu.ac.kr
4 Department of Chemistry, School of Materials Science and Engineering, Gwangju Institute of Science and Technology, 123 Cheomdan-gwagiro, Buk-gu, Gwangju 61005, Korea
* Correspondence: shong@gist.ac.kr; Tel.: +82-62-715-2346

Received: 15 June 2020; Accepted: 6 July 2020; Published: 8 July 2020

Abstract: Nickel(II) dichloride complexes with a pyridine-chelated imidazo[1,5-*a*]pyridin-3-ylidene py-ImPy ligand were developed as novel catalyst precursors for acrylate synthesis reaction from ethylene and carbon dioxide (CO_2), a highly promising sustainable process in terms of carbon capture and utilization (CCU). Two types of ImPy salts were prepared as new C,N-bidentate ligand precursors; py-ImPy salts (**3**, **4a**–**4e**) having a pyridine group at C(5) on ImPy and a *N*-picolyl-ImPy salt (**10**) having a picolyl group at N atom on ImPy. Nickel(II) complexes such as py-ImPyNi(II)Cl_2 (**7**, **8a**–**8e**) and *N*-picolyl-ImPyNi(II)Cl_2 (**12**) were synthesized via transmetalation protocol from silver(I) complexes, py-ImPyAgCl (**5**, **6a**–**6e**) and *N*-picolyl-ImPyAgCl (**11**). X-ray diffraction analysis of nickel(II) complexes (**7**, **8b**, **12**) showed a monomeric distorted tetrahedral geometry and a six-membered chelate ring structure. py-ImPy ligands formed a more planar six-membered chelate with the nickel center than did *N*-picolyl-ImPy ligand. py-ImPyNi(II)Cl_2 complexes (**8a**–**8e**) with *tert*-butyl substituents exhibited noticeable catalytic activity in acrylate synthesis from ethylene and CO_2 (up to 108% acrylate). Interestingly, the use of additional additives including monodentate phosphines increased catalytic activity up to 845% acrylate (TON 8).

Keywords: nickel; silver; *N*-heterocyclic carbene; bidentate ligands; acrylate; ethylene; carbon dioxide

1. Introduction

The synthesis of acrylic acid derivatives through the C–H carboxylation of ethylene with carbon dioxide (CO_2) has received much attention lately in the area of carbon capture and utilization (CCU) [1–11], as the acrylate products are value-added chemicals for superabsorbent polymers, adhesives, and coatings. This new acrylate synthetic route could be superior to the existing industrial process (two-stage oxidation of propylene) by utilizing less expensive feedstock (ethylene vs. propylene) and a sustainable carbon source (CO_2) [12].

In pioneering studies in the 1980s, Hoberg [13–17] and Carmona [18–20] independently reported metal (Ni, Fe, Mo, W) mediated stoichiometric coupling reactions between ethylene and CO_2. Hoberg demonstrated that oxidative coupling of ethylene and CO_2 proceeded smoothly to afford nickelalactone products by

electron-rich Ni(0) complexes ligated with 2,2′-bipyridine (bpy), bis(dicyclohexylphosphino)ethane (DCPE), 1,8-diazabicyclo(5,4,0)undec-7-ene (DBU), and pyridyl-phosphine ligands. These stoichiometric reaction results inspired researchers to develop a catalytic version; however, the development of catalytic processes turned out to be highly challenging [21–27]. Turning over the proposed catalytic cycle was impeded by the high energy barrier for β-hydride elimination of stable five-membered nickelalactones and the endergonic thermodynamic feature of the overall reaction (ethylene + CO_2 → acrylic acid) [28–31]. After three decades, the long-standing problem was nicely solved by Vogt [32] and Limbach [33,34], independently. Nickel-catalyzed C–H carboxylation of ethylene using CO_2 was successfully realized by the cleavage of the nickelalactone using either hard Lewis acid [32] or strong alkoxide bases [33,34] (Figure 1a). Since then, studies on nickel (Ni)–Catalysis with extensive ligand screening have demonstrated that the choice of ligands greatly affects the catalytic activity, and electron-rich bisphosphine ligands are often preferred for catalytic efficiency [35–38]. Recently, several attempts have been made to extend the catalysis to metals other than Ni, including Pd [35,39–41], Co [42], Ru [43], and Fe [44]. Despite progress in recent years, there remains a long road ahead for an industrial application; therefore, more diverse ligands and metals should be explored to develop a highly efficient catalytic acrylate synthesis process using ethylene and CO_2 [45–47].

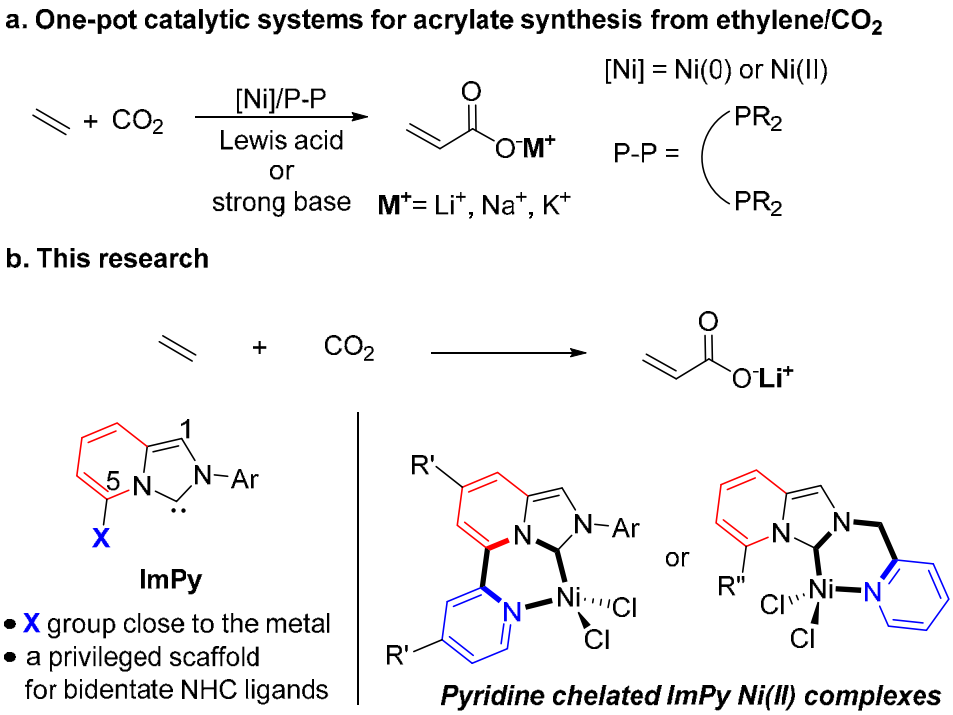

Figure 1. (**a**) One-pot catalytic systems for acrylate synthesis from ethylene and CO_2 [32–34]; (**b**) this research: pyridine chelated ImPy Ni(II) complexes for acrylate synthesis from ethylene and CO_2.

As part of our research interests in the design and application of *N*-heterocyclic carbenes (NHCs) [48–55], we were intrigued by the ideas of exploring various bidentate NHC ligands in the Ni-catalyzed C–H carboxylation reaction of ethylene with CO_2. NHCs are strong electron-donating and highly versatile ligands. The use of NHC ligands has resulted in breakthroughs in many catalytic reactions, such as ruthenium-based olefin metathesis [56–64]. Furthermore, bidentate NHC ligand systems could provide more stable complexes by the chelate effect and expand the scope of the catalytic transformations [65–70]. Nevertheless, there has been one example where NHC ligands are used in the synthesis of acrylate from CO_2/ethylene [47].

In 2005, Glorius and Lassaletta independently developed imidazo [1,5-*a*] pyridine-3-ylidene (ImPy) ligands, classified as the rigid heterobicyclic variant of NHCs [71,72]. A substituent at C(5) on the bicyclic ImPy can be placed adjacent to a metal coordination sphere, often forming bonding interactions

with the metal [73–90]. For that reason, ImPys have attracted much attention as a privileged scaffold for bidentate NHC ligands [81–90]. Recently, Nozaki reported Ni and Pd complexes having C,X-bidentate ImPy ligands (X = phenoxide [84,85,88] and phosphine oxide [86]), which efficiently catalyzed ethylene polymerization and copolymerization with polar monomers. More recently, Wang reported Pd complexes bearing chelating ImPy-sulfonate ligand for norbornene polymerization [89]. Thus, we envisioned that the transition-metal complexes containing a C,X-bidentate ImPy ligand could also be effective for the catalytic synthesis of acrylate from CO_2/ethylene.

Pyridine ligands are known as active ligands for nickel promoted coupling reactions using ethylene and CO_2 [13,17,91–93], which inspired us to develop mononuclear Ni(II) complexes containing a pyridine-chelated ImPy for catalytic acrylate synthesis from CO_2/ethylene (Figure 1b). We herein present novel mononuclear Ni(II) complexes with a rigid six-membered ring, imposed by a special pyridine-chelated bidentate ImPy ligand, providing catalytic activity in the acrylate formation from ethylene and CO_2.

2. Results and Discussion

2.1. Synthesis of Ligand Precursors

Two types of pyridine-chelated ImPy ligand precursors were synthesized: (i) py-ImPy^R salts (R = H **3** and R = *t*-Bu **4a**–**4e**) with a pyridine group at C(5) on ImPy, and (ii) a *N*-picolyl-ImPy salt (**10**) with a picolyl group at N on ImPy (Scheme 1). The py-ImPy^R salts (**3**, **4a**–**4e**) were obtained in moderate yields (67%–85%), through iminopyridine formation from 2,2′-bipyridine-6-carbaldehyde derivatives (**1**–**2**) and anilines (Ar–NH_2), followed by the cyclization with chloromethylethyl ether. The lack of substituents on pyridine and ImPy units of py-ImPy^H salt (**3**) lead to the formation of less soluble Ni complex. Therefore, the *tert*-butyl substituents were introduced into the backbone of the ligand to improve the solubility, hence delivering py-ImPy$^{t\text{-Bu}}$ salts (**4a**–**4e**) [94–96]. The *N*-picolyl-ImPy salt (**10**) was synthesized in 63% yield through the condensations of corresponding aldehyde (**9**), 2-picolylamine, and paraformaldehyde [97].

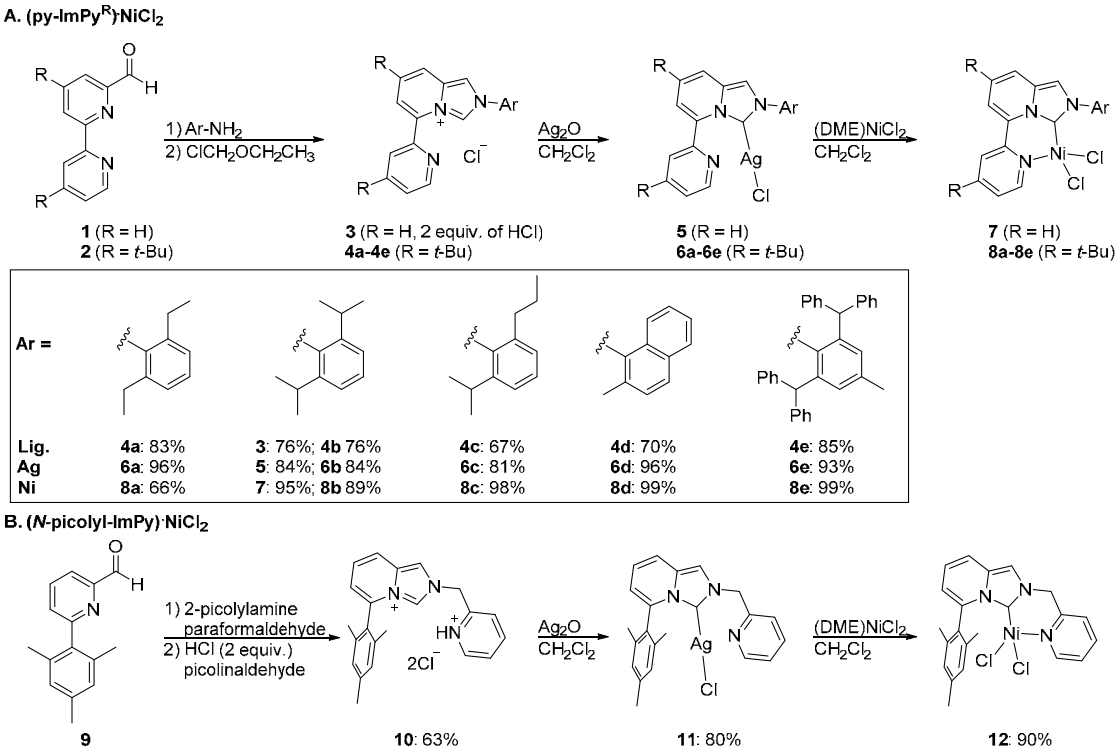

Scheme 1. Synthesis of ligand precursors, Ag complexes, and Ni complexes.

2.2. Synthesis and Structural Analysis of Ag(I) Complexes

Synthesized ligand precursors were converted to silver (Ag) complexes that could serve useful transmetallating agents for Ni complexes (Scheme 1). Ag(I) complexes (**5**, **6a**–**6e**, **11**) were prepared from the imidazopyridinium salts (**3**, **4a**–**4e**, **10**) by reaction with Ag(I) oxide in good yields (81%–96%) (Scheme 1). After the disappearance of peaks related to the acidic imidazopyridinium proton of **3**, **4a**–**4e**, and **10** were confirmed in ^{1}H NMR, Ag complexes were purified by washing with hexane or recrystallization from CH_2Cl_2 and hexanes. The molecular structure of an Ag complex **5** was characterized by X-ray crystallography (Figure 2). A single crystal for X-ray diffraction was prepared by slow recrystallization from dichloromethane layered with hexane. The crystal structure exhibited a mononuclear Ag(I) complex with a linear geometry, which is attributed to the unique steric effect at C(5) on the ImPy. Similar structural features were observed in other previously reported Ag(I) chloride complexes with ImPy [98].

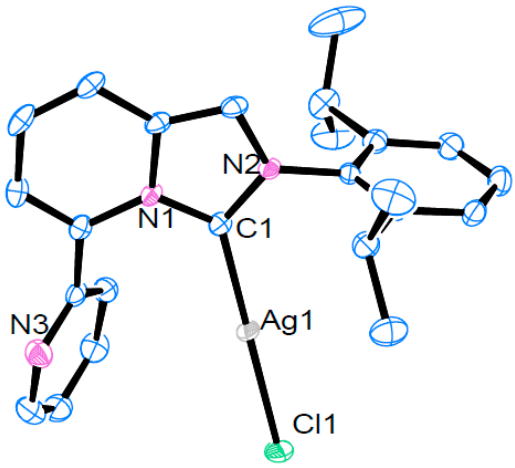

Figure 2. Molecular structure of **5**. Thermal ellipsoids are set at 50% probability. Hydrogen atoms have been omitted for clarity.

2.3. Synthesis and Structural Analysis of Nickel(II) Complexes

ImPy Ag(I) complexes (**5**, **6a**–**6e**, **11**) were employed for subsequent transmetalation with (DME)$NiCl_2$ (DME as dimethoxyethane) to afford Ni(II) complexes (**7**, **8a**–**8e**, **12**) in up to 99% yield (Scheme 1). All complexes were analyzed by elemental analysis and UV spectroscopy. Ni complexes could not be analyzed by NMR spectroscopy owing to their paramagnetic properties. Magnetic susceptibility in the solid-state was measured by magnetic susceptibility balance. Effective magnetic moments (μ_{eff} = 2.56–3.09 BM, 297 K) were found to be similar to the spin-only value (2.87 BM, S = 1) [99], which demonstrates that the Ni(II) complexes are paramagnetic species, high-spin d^8 ions with two unpaired electrons.

Structural characterization of **7**, **8b**, and **12** were established by X-ray crystallography. Single crystals of **7**, **8b**, and **12** suitable for X-ray diffraction analysis were grown through the slow diffusion of *n*-hexane into a saturated solution of dichloromethane. Three complexes were observed as desired monomeric Ni(II) complexes with four-coordinated species (Figures 3–5). The Ni(II) center displays a distorted tetrahedral geometry. The most remarkable structural feature of **7**, **8b**, and **12** is the coordination of the carbene carbon and pyridine nitrogen (N) to the Ni(II) center, displaying a bidentate C, N chelating mode that yields a six-membered nickelacycle.

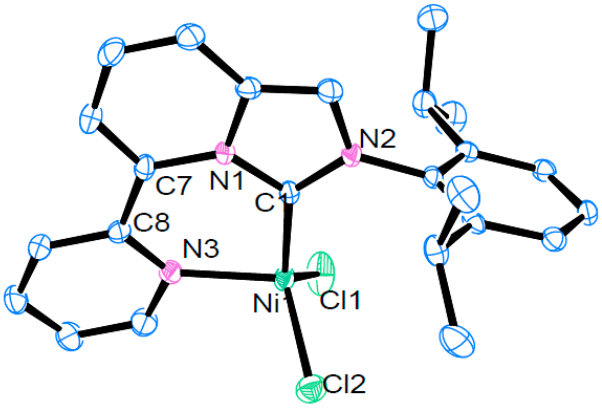

Figure 3. Molecular structure of **7**. Thermal ellipsoids are set at 50% probability. Hydrogen atoms have been omitted for clarity. Selected bond lengths [Å] and angles [°]: Ni(1)–C(1) 1.937(2), Ni(1)–N(3) 2.008(2), Ni(1)–Cl(1) 2.2077(8), Ni(1)–Cl(2) 2.2439(7); C(1)–Ni(1)–N(3) 92.84(9). Selected torsion angles [°]: C(1)–N(1)–C(7)–C(8) -1.1(4), N(1)–C(7)–C(8)–N(3) -8.4(3), C(7)–C(8)–N(3)–Ni(1) 15.6(3), C(8)–N(3)–Ni(1)–C(1) -11.7 (2), N(3)–Ni(1)–C(1)–N(1) 2.4(2), Ni(1)–C(1)–N(1)–C(7) 2.7 (3).

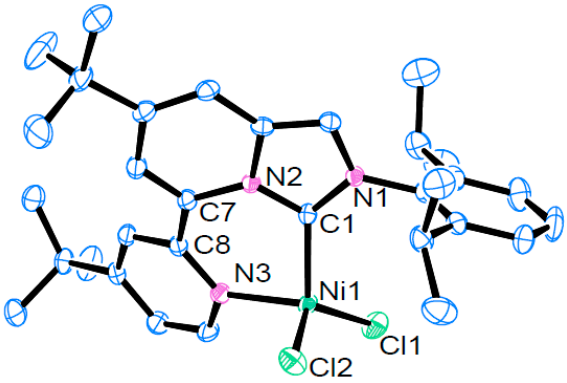

Figure 4. Molecular structure of **8b**. Thermal ellipsoids are set at 50% probability. Hydrogen atoms have been omitted for clarity. Selected bond lengths [Å] and angles [°]: Ni(1)–C(1) 1.947(2), Ni(1)–N(3) 2.015(1), Ni(1)–Cl(1) 2.2124(6), Ni(1)–Cl(2) 2.2377(6); C(1)–Ni(1)–N(3) 91.83(6). Selected torsion angles [°]: C(1)–N(2)–C(7)–C(8) -15.8(2), N(2)–C(7)–C(8)–N(3) 32.0(2), C(7)–C(8)–N(3)–Ni(1) -10.7(2), C(8)–N(3)–Ni(1)–C(1) -16.4(1), N(3)–Ni(1)–C(1)–N(2) 30.8(1), Ni(1)–C(1)–N(2)–C(7) -20.3(2).

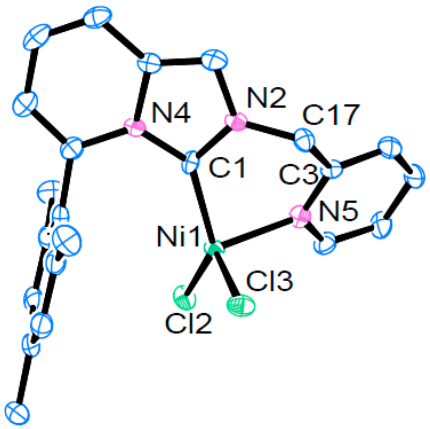

Figure 5. Molecular structures of **12**. Thermal ellipsoids are set at 50% probability. Hydrogen atoms have been omitted for clarity. Selected bond lengths [Å] and angles [°]: Ni(1)–C(1) 1.991(9), Ni(1)–N(5) 2.047(8), Ni(1)–Cl(2) 2.224(2), Ni(1)–Cl(3) 2.273(3); C(1)–Ni(1)–N(5) 92.0(3). Selected torsion angles [°]: C(1)–N(2)–C(17)–C(3) 57(1), N(2)–C(17)–C(3)–N(5) -51(1), C(17)–C(3)–N(5)–Ni(1) 3(1), C(3)–N(5)–Ni(1)–C(1) 30.4(7), N(5)–Ni(1)–C(1)–N(2) -26.7(7), Ni(1)–C(1)–N(2)–C(17) -10(1).

The Ni–C1 bonds of **7** and **8b** complexes have lengths of 1.937(2) and 1.947(2) Å, respectively, which are 0.04~0.05 Å shorter than that of **12** (1.991(9)). The bond lengths between the Ni and the N donors in **7** and **8b** complexes are 2.008(2) and 2.015(1) Å, respectively—that is, ~0.03–0.04 Å shorter than that of **12** (2.047(8)). The bidentate py-ImPy ligands result in acute bite angles of 92.84(9)°, 91.83(6)° and 92.0(3)° in **7**, **8b** and **12**, respectively (vs. 109.5° in tetrahedral geometry), and inclinations of the Ni(1)–C(1) bond by 3.2°, 16.4° and 9.8°, respectively, to the axis defined by the centroid of the imidazole plane and the carbene carbon atom C1 [87,100].

The torsion angles of C(1)–N(1)–C(7)–C(8) and N(1)–C(7)–C(8)–N(3) in **7** are −1.1° and −8.4°, respectively, while those of C(1)–N(2)–C(7)–C(8) and N(2)–C(7)–C(8)–N(3) in **8b** are −15.8° and 32.0°, respectively (Figures 3 and 4). They are smaller than those of **12**, which are 57° and −51°, respectively (Figure 5). Note that py-ImPy ligands containing aromatic N-fused heterobicyclic skeletons contain more rigid six-membered chelate rings than that by *N*-picolyl-ImPy ligand, thus showing a stronger chelating effect.

2.4. Nickel Mediated Acrylate Synthesis from Ethylene Using CO_2

Newly prepared ligand precursors (**3**, **4a**–**4e**, **10**) were tested in the "in-situ" Ni(II)-mediated C-H carboxylation of ethylene using CO_2, which was modified from Vogt's reaction conditions (Scheme S1). Interestingly, the activities (up to 50% acrylate) were observed only for the py-ImPy^R ligand salts (**3**, **4a**–**4e**) bearing the pyridine chelating group at the C(5) position. On the other hand, no acrylate product was observed when non-pyridine bidentate ImPy ligand precursors were used, for example, bis-ImPy, OMe-ImPy, and O = P-ImPy. Moreover, no acrylate was detected when typical monodentate NHC ligands were used such as ImPy·HCl or IPr·HCl. Although the ligand screening using the in situ generation method might not accurately reflect the inherent ability of the ligands to promote the reaction, it could provide a reasonable starting point to develop as novel carbene ligands for the C-H carboxylation reaction.

We then examined whether the isolated Ni(II) complexes (**7**, **8a–8b**, **12**) could yield lithium acrylates under similar reaction conditions (Table 1). We were pleased to find that **7**, **8b** showed better yields than that of **12** (entry **1**, **3** vs. entry **7**). In particular, **8b** bearing *tert*-butyl substituents on the py-ImPy backbone yielded lithium acrylate in slightly stoichiometric amounts (entries 2–6, up to 80% acrylate). The ligand sterics are known to affect the catalytic performance in ethylene–CO_2 coupling reaction (entries 19–20) [32,36]. Thus, we have further varied the ligand structure of the Ni(II) complexes (**8a**, **8c–8e**) by modulating the aniline unit of the Ni complex **8b**. Overall, Ni(II) complexes having *tert*-butyl pyridine units (**8a–8e)** showed higher efficiency than that of complex **7** without *tert*-butyl groups. The activity of complex **8a** having a smaller 2,6-diethylphenyl group was similar to that of **8b** having the 2,6-diisopropylphenyl group (entry **2** vs. entry **3**). Complex **8c** replacing an isopropyl group on the aryl ring with *n*-propyl group afforded a slightly over-stoichiometric yield (entry 4, 108% acrylate, TON 1). The complexes having a methylnaphthalenyl group (**8d**) or very bulky 2,6-$(Ph_2CH)_2$-4-Me-C_6H_2 group (**8e**) showed relatively low activity (entries **5**–**6** vs. entry **3**). These results might suggest that reactivity could be related to the stronger chelating effect by a more rigid and planar six-membered chelate ring (Figure 3).

Table 1. Isolated Ni(II) complexes for Ni mediated acrylate synthesis.

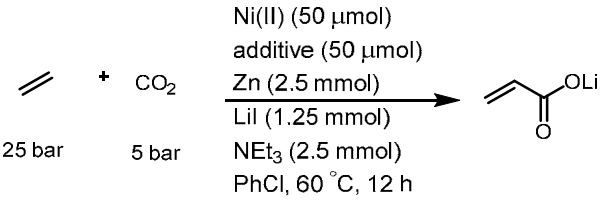

Entry	Ni(II)	Additives	% Acrylate [a]
1	**7**	none	34
2	**8a**	none	85
3	**8b**	none	80
4	**8c**	none	108
5	**8d**	none	50
6	**8e**	none	62
7	**12**	none	n/a [b]
8	**7**	PCy_3	180
9	**8a**	PCy_3	677
10	**8b**	PCy_3	845
11	**8c**	PCy_3	728
12	**8d**	PCy_3	194
13	**8e**	PCy_3	814
14	$(DME)NiCl_2$	PCy_3	n/a [b]
15 [c]	$(DME)NiBr_2$	DPPE	1200
16 [c]	$(DME)NiBr_2$	DCPE	1500
17 [c]	$(DME)NiBr_2$	DPPP	900
18 [c]	$(DME)NiBr_2$	DCPP	1000
19 [d]	$Ni(COD)_2$	DCPE	800
20 [e]	$Ni(COD)_2$	DCPP	1400
21 [c]	$(DME)NiBr_2$	bpy	0
22 [c]	$(DME)NiBr_2$	Dtbbpy	0

[a] % acrylate was determined by ^1H NMR spectroscopy using sodium 3-(trimethylsilyl)-2,2,3,3-d_4-propionate as the internal standard. % acrylate = (mmol acrylate)/(mmol Ni) × 100; [b] acrylate peaks could not be reliably integrated; [c] 20 h; [d] Reference [36]: 50 °C, 24 h; [e] Reference [32]: 50 °C, 72 h.

In an effort to improve the yield of acrylate, we were intrigued by the idea of adding monodentate phosphines (Scheme S2). It has been reported that phosphines could prevent catalyst decomposition in the reaction for acrylate formation [40,101]. Certain monodentate phosphines, like PCy_3, were proved to be beneficial, as catalytic activities of up to 845% acrylate (TON of 8.4) were demonstrated (entries 8–13). It is interesting to note that in the absence of py-ImPy ligand, PCy_3 alone did not show reactivity (entry 14). As a reference point, the bidentate bisphosphine ligands such as bis(diphenylphosphino)ethane (DPPE), DCPE, bis(diphenylphosphino)propane (DPPP) and bis(dicyclohexylphosphanyl)propane (DCPP) were performed with $(DME)NiBr_2$ in the similar reaction conditions (entries 15–18, Scheme S3), as they are known to be good ligands in the literature (entries 19–20) [32–38]. Although bipyridines have been known as potential ligands for Ni-mediated oxidative coupling of CO_2 and ethylene [13], typical bipyridine ligands such as bpy and 4,4′-di-*tert*-butyl-2,2′-dipyridine (Dtbbpy) were entirely ineffective (entries 21–22). Thus, the activity was only observed for the ImPy ligands bearing the pyridine chelating group at the C(5) position. It was found that the reactivity of the most active catalysts, such as **8b**/PCy_3 (TON 8), is comparable to those of $(DME)NiBr_2$/DPPP (TON 9) and $Ni(COD)_2$/DCPP(TON 14).

*2.5. Optimization of Reaction Conditions Using the Combination **8b** and PCy_3*

To optimize the reaction conditions for acrylate synthesis using the combination of **8b** and PCy_3, we have systematically varied several parameters, including the base and the solvent (Table 2). The role of Et_3N in the lithium acrylate synthesis helps to remove HI generated during the reaction, which is known to be similar to the role in Ni Heck-type reaction [32]. Therefore, several weak bases to abstract HI,

such as diisopropylethylamine (DIPEA), pyridine (py), K_2CO_3, Cs_2CO_3, 1,4-diazabicyclo [2.2.2] octane (DABCO), and tetramethylethylenediamine (TMEDA), were screened (entries 2–7). Among them, only organic bases, such as DIPEA and pyridine, showed reactivities, but these were significantly lower than that of Et_3N (entries 2–3). Strong alkoxide bases such as sodium 2-fluorophenoxide (2-F-PhONa), sodium 2,6-dimethylphenoxide (2,6-Me-PhONa) and *t*-BuOK did not produce any acrylate (entries 8–12) [33,34]. In addition, the sodium iodide (NaI) did not produce the product (entry 13). Therefore, Et_3N/LiI was chosen for the next catalysis experiments. Subsequently, we investigated the effect of solvents on the acrylate synthesis (entries 14–21). First, we screened weakly coordinating solvents such as toluene, anisole, benzene, and 2-chlorotoluene (2-Cl-Tol), as they are effective solvents reported in the Vogt's system [32,42]. Although these solvents were suitable in acrylate synthesis (54%–799% acrylate), PhCl is still the most effective solvent. Next, screening of other solvents such as THF, CH_2Cl_2, DMF and 1,4-dioxane did not give any acrylate, suggesting that more strongly coordinating solvents could hinder the weakly binding substrate from coordinating to the metal center [32]. The reaction performed without Zn did not proceed, confirming the importance of Zn as a reducing agent (entry 22). Et_3N base and weakly coordinating solvents that were favored in the Vogt conditions, are also effective in this system [32].

Table 2. Reaction optimization for Ni-catalyzed acrylate synthesis from ethylene and CO_2.

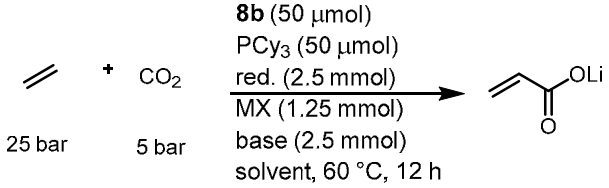

Entry	Base	Solvent	Red.	MX	% Acrylate [a]
1	NEt_3	PhCl	Zn	LiI	845
2	DIPEA	PhCl	Zn	LiI	34
3	py	PhCl	Zn	LiI	80
4	K_2CO_3	PhCl	Zn	LiI	0
5	Cs_2CO_3	PhCl	Zn	LiI	0
6	DABCO	PhCl	Zn	LiI	0
7	TMEDA	PhCl	Zn	LiI	0
8	2-F-PhONa	PhCl	Zn	-	0
9	2,6-Me-PhONa	PhCl	Zn	-	0
10	2,6-Me-PhONa	PhCl	Zn	NaI	0
11	*t*-BuOK	PhCl	Zn	-	0
12	*t*-BuOK	PhCl	Zn	LiI	0
13	NEt_3	PhCl	Zn	NaI	0
14	NEt_3	toluene	Zn	LiI	54
15	NEt_3	anisole	Zn	LiI	416
16	NEt_3	benzene	Zn	LiI	85
17	NEt_3	2-Cl-Tol	Zn	LiI	799
18	NEt_3	THF	Zn	LiI	0
19	NEt_3	CH_2Cl_2	Zn	LiI	0
20	NEt_3	DMF	Zn	LiI	0
21	NEt_3	1,4-dioxane	Zn	LiI	0
22	NEt_3	PhCl	-	LiI	0

[a] % acrylate was determined by ^{1}H NMR spectroscopy using sodium 3-(trimethylsilyl)-2,2,3,3-d_4-propionate as an internal standard. % acrylate = (mmol acrylate)/(mmol Ni) × 100.

3. Materials and Methods

3.1. General Remarks

All air- and moisture-sensitive reactions were performed under an argon atmosphere either using Schlenk techniques or a glove box. All reactions involving the formation of acrylate from

ethylene and CO_2 were carried out in 100 mL stainless steel autoclaves (Hanwoul Engineering Co., Gunpo-si, Republic of Korea). Nuclear magnetic resonance (NMR) (JEOL, Tokyo, Japan) spectra were recorded on a JEOL 400 spectrometer, operated at 400 MHz for ^{1}H NMR and at 100 MHz for ^{13}C NMR. Chemical shifts (ppm) for ^{1}H were referenced to the residual solvent peak ($CDCl_3$ = δ 7.26 ppm, CD_2Cl_2 = δ 5.32 ppm, CD_3OD = δ 3.31 ppm, $(CD_3)_2SO$ = 2.50 ppm, D_2O = δ 4.79 ppm). Multiplicities were recorded as s (singlet), d (doublet), t (triplet), q (quartet), sept (septet), or m (multiplet). Chemical shifts (ppm) for ^{13}C were referenced relative to the residual solvent peak (CD_2Cl_2 = δ 53.84 ppm, CD_3OD = δ 49.00 ppm, $(CD_3)_2SO$ = 39.52 ppm). High-resolution mass spectra (HRMS) were recorded on a JEOL JMS-700 MStation mass spectrometer (JEOL, Tokyo, Japan). Elemental analyses were carried out with an UNICUBE Elemental Analyzer (Elementar, Langenselbold, Germany). The magnetic susceptibilities of nickel complexes were measured in the solid state using a magnetic susceptibility balance (Sherwood Scientific, Cambridge, UK). Diamagnetic corrections were ignored. UV/vis measurements of nickel complexes were carried out in CH_2Cl_2 solution using a Perkin-Elmer UV/VIS NIR Spectrometer Lambda 950 (Perkin Elmer, Shelton, USA). Analytical thin layer chromatography (TLC) (Merck KGaA, Darmstadt, Germany) was performed with Merck pre-coated silica gel 60 Å (F254) glass plates and visualization on TLC was achieved by UV light. Flash chromatography was performed with 230–400 Mesh 60 Å Silica Gel purchased from Merck Inc.

3.2. Materials

Ethylene gas (99.999%) and carbon dioxide (99.99%) were purchased from Sinil Gas Co. Ethylene was purified by passing through a column packed with BASF catalyst R3–11G, activated carbon and 4 Å molecular sieves. Carbon dioxide was dried by passing through a column packed with 4 Å molecular sieves. All the chemicals were purchased from Aldrich, Acros, TCI, or Alfa-Aesar Chemical Co. and used as received unless otherwise noted. Anhydrous tetrahydrofuran (THF), diethyl ether (Et_2O), dichloromethane (CH_2Cl_2) and dimethylformamide (DMF) were dried using a J.C. Meyer solvent purification system. Triethyl amine, toluene and hexane were distilled from calcium hydride. 2-Picolyl amine and 2,6-diisopropylaniline were distilled via short path distillation. Methanol and ethanol were dried over 4 Å molecular sieves. The following compounds were prepared based on the original and/or modified procedures: 2,2′-bipyridine-6-carbaldehyde **1** [102], 4,4′-di-tert-butyl-6-methyl-2,2′-bipyridine **2** [92], 6-mesityl-pyridine-2-carboxaldehyde **9** [103], 2-isopropyl-6-propylaniline [104], and 2,6-dibenzhydryl-4-methylaniline [105].

3.3. Synthesis of Ligand Precursors. General Procedure

Aldehyde (1 equiv), aniline (1–1.05 equiv) and ethanol or methanol (0.1–0.2 M) were added to a Schlenk flask equipped with a magnetic stirrer and sealed with a rubber septum tightened with a cable tie. The mixture was stirred at 90 °C for 24–48 h. The solvent was removed under reduced pressure. If needed, the crude was purified by basic column chromatography. Then, imine derivatives were transferred to a Schlenk tube equipped with a Teflon-valve. The solvent was removed by blowing nitrogen gas and using vacuum. Subsequently, chloromethyl ethyl ether (20 equiv) was added and stirred at 90 °C. After cooling to room temperature, the volatiles were removed by rotary evaporation and recrystallization with dichloromethane and hexane. The crude solids were purified through flash column chromatography and recrystallization with dichloromethane and hexane.

2-(2,6-diisopropylphenyl)-5-(pyridin-1-ium-2-yl)-2H-imidazo[1,5-*a*]pyridinium dichloride (3): Following the general procedure of ligand precursors, a product **3** (172 mg, 76% yield) was obtained as white solid from 2, 2′-bipyridine-6-carbaldehyde **1** (98 mg, 0.53 mmol), 2,6-diisopropylaniline (0.10 mL, 0.53 mmol), formic acid (1 drop), methanol (5 mL) and chloromethyl ethyl ether (1 mL, 10.6 mmol). The cyclization of imine derivative with chloromethyl ethyl ether was completed in 3 days. The crude product was purified through flash column chromatography (CH_2Cl_2:CH_3OH = 8:1). ^{1}H NMR (400 MHz, CD_2Cl_2) δ 10.66 (d, *J* = 1.8 Hz, 1H), 8.71 (s, 2H), 8.53 (d, *J* = 9.1 Hz, 1H), 8.25 (d, *J* = 8.2 Hz,

1H), 8.09–8.01 (m, 2H), 7.70–7.61 (m, 2H), 7.51 (dd, *J* = 7.6, 4.9 Hz, 1H), 7.43 (d, *J* = 7.8 Hz, 2H), 2.22 (sept, *J* = 7.3 Hz, 2H), 1.23 (d, *J* = 6.8 Hz, 6H), 1.18 (d, *J* = 6.8 Hz, 6H). ^{13}C NMR (100 MHz, CD_2Cl_2) δ 150.36, 149.00, 145.44, 138.65, 132.79, 132.67, 132.33, 131.17, 127.33, 125.93, 125.38, 124.92, 123.86, 121.28, 120.52, 117.83, 54.38, 54.11, 53.84, 53.57, 53.30, 28.95, 24.39, 24.35 HR-MS (FAB): calcd. for $C_{24}H_{26}N_3$ [M-H-2Cl] 356.2127 found 356.2119. Elemental analysis (%) calcd. for $C_{24}H_{27}Cl_2N_3$: C, 67.29; H, 6.35; N, 9.81. Found: C, 67.33; H, 6.51; N, 9.75.

7-(tert-butyl)-5-(4-(tert-butyl)pyridin-2-yl)-2-(2,6-diethylphenyl)-2,3-dihydroimidazo[1,5-*a*] pyridinium chloride (4a): Following the general procedure of ligand precursors, a product **4a** (265 mg, 83% yield) was obtained as a beige solid from 4,4′-di-tert-butyl-[2,2′-bipyridine]-6-carbaldehyde **2** (200 mg, 0.67 mmol), 2,6-diethylaniline (0.10 mL, 0.67 mmol), ethanol (3.4 mL) and chloromethyl ethyl ether (1.25 mL, 13.4 mmol). The cyclization of imine derivative with chloromethyl ethyl ether was completed in 24 h. The crude product was purified through flash column chromatography (CH_2Cl_2:AcOEt:CH_3OH = 4.5:0.5:0.5). ^{1}H NMR (400 MHz, CD_2Cl_2) δ 10.28 (d, *J* = 1.7 Hz, 1H), 8.76 (d, *J* = 1.9 Hz, 1H), 8.62 (d, *J* = 5.3 Hz, 1H), 8.34 (d, *J* = 1.1 Hz, 1H), 7.92 (d, *J* = 1.6 Hz, 1H), 7.69 (d, *J* = 1.7 Hz, 1H), 7.56 (t, *J* = 7.8 Hz, 1H), 7.51 (dd, *J* = 5.3, 1.7 Hz, 1H), 7.35 (d, *J* = 7.8 Hz, 2H), 2.43–2.18 (m, 4H), 1.47 (s, 9H), 1.44–1.39 (m, 9H), 1.14 (t, *J* = 7.6 Hz, 6H). ^{13}C NMR (100 MHz, CD_2Cl_2) δ 163.10, 150.58, 149.34, 149.07, 140.77, 133.40, 133.09, 133.03, 131.97, 127.53, 126.38, 122.97, 120.56, 119.37, 116.68, 114.95, 54.38, 54.11, 53.84, 53.57, 53.30, 35.66, 35.50, 30.53, 30.08, 24.35, 15.25. HR-MS (FAB): calcd. for $C_{30}H_{38}N_3$ [M-Cl] 440.3066 found 440.3068. Elemental analysis (%) calcd. for $C_{30}H_{38}ClN_3$: C, 75.68; H, 8.05; N, 8.83. Found: C, 75.42; H, 8.301; N, 8.61.

7-(tert-butyl)-5-(4-(tert-butyl)pyridin-2-yl)-2-(2-isopropyl-6-propylphenyl)-2,3-dihydroimidazo [1,5-*a*]pyridinium chloride (4c): Following the general procedure of ligand precursors, a product 4c (228 mg, 67% yield) was obtained as white solids from 4,4′-di-tert-butyl-[2,2′-bipyridine]-6-carbaldehyde 2 (200 mg, 0.67 mmol), 2-isopropyl-6-propylaniline (119 mg, 0.67 mmol), ethanol (3.4 mL) and chloromethyl ethyl ether (1.25 mL, 13.4 mmol). The cyclization of imine derivative with chloromethyl ethyl ether was completed in 24 h. The crude product was purified through flash column chromatography (hexane:AcOEt:CH_3OH = 3.5:0.5:0.5). ^{1}H NMR (400 MHz, CD_2Cl_2) δ δ 10.26 (s, 1H), 8.71 (d, *J* = 1.9 Hz, 1H), 8.61 (dd, *J* = 5.3, 0.8 Hz, 1H), 8.33 (s, 1H), 7.94 (dd, *J* = 1.8, 0.7 Hz, 1H), 7.71 (d, *J* = 1.8 Hz, 1H), 7.58 (t, *J* = 7.8 Hz, 1H), 7.51 (dd, *J* = 5.3, 1.8 Hz, 1H), 7.40 (dd, *J* = 7.9, 1.4 Hz, 1H), 7.31 (dd, *J* = 7.7, 1.4 Hz, 1H), 2.31–2.15 (m, 3H), 1.60–1.52 (m, 2H), 1.48 (s, 9H), 1.42 (s, 9H), 1.21 (d, *J* = 6.8 Hz, 3H), 1.15 (d, *J* = 6.8 Hz, 3H), 0.83 (t, *J* = 7.3 Hz, 3H). ^{13}C NMR (100 MHz, CD_2Cl_2) δ 163.12, 150.54, 149.30, 149.20, 145.63, 139.21, 133.37, 133.01, 132.27, 131.98, 128.01, 126.54, 125.09, 122.99, 120.52, 119.44, 116.81, 114.89, 35.68, 35.51, 33.20, 30.52, 30.08, 28.88, 24.42, 24.40, 24.34, 13.98. HR-MS (FAB): calcd. for $C_{32}H_{42}N_3$ [M-Cl] 468.3379 found 468.3377. Elemental analysis (%) calcd. for $C_{32}H_{42}ClN_3$: C, 76.24; H, 8.4; N, 8.33. Found: C, 76.34; H, 8.749; N, 8.22.

7-(tert-butyl)-5-(4-(tert-butyl)pyridin-2-yl)-2-(2-methylnaphthalen-1-yl)-2,3-dihydroimidazo [1,5-*a*] pyridinium chloride (4d): Following the general procedure of ligand precursors, a product **4d** (227 mg, 70% yield) was obtained as white solids from 4,4′-di-tert-butyl-[2,2′-bipyridine]-6-carbaldehyde **2** (200 mg, 0.67 mmol), 2-methylnaphthalen-1-amine (105 mg, 0.67 mmol), ethanol (3.4 mL) and chloromethyl ethyl ether (1.25 mL, 13.4 mmol). The cyclization of imine derivative with chloromethyl ethyl ether was completed in 2 days. Then, the crude product was purified through flash column chromatography (hexane:AcOEt:CH_3OH = 3.5:0.5:0.5). ^{1}H NMR (400 MHz, CD_2Cl_2) δ 10.41 (s, 1H), 8.87 (s, 1H), 8.57 (d, *J* = 5.3 Hz, 1H), 8.42 (s, 1H), 8.07 (d, *J* = 8.5 Hz, 1H), 7.98 (d, *J* = 7.3 Hz, 1H), 7.93 (d, *J* = 1.2 Hz, 1H), 7.73 (s, 1H), 7.52 (m, 4H), 7.03 (d, *J* = 8.3 Hz, 1H), 2.30 (s, 3H), 1.48 (s, 9H), 1.40 (s, 9H). ^{13}C NMR (100 MHz, CD_2Cl_2) δ 162.99 (s), 150.56 (s), 149.31, 149.12, 133.91 (s), 133.49, 133.31, 132.62 (s), 131.69 (s), 129.66, 129.57, 129.03 (s), 128.63, 128.59, 127.04 (s), 126.79 (s), 122.87 (s), 120.63, 120.61, 119.41 (s), 116.96 (s), 114.97 (s), 35.63 (s), 35.42 (s), 30.47 (s), 30.05 (s), 17.98 (s). HR-MS (FAB): calcd. for $C_{31}H_{34}N_3$ [M-Cl] 448.2753 found 448.2751. Elemental analysis (%) calcd. for $C_{31}H_{34}ClN_3$: C, 76.92; H, 7.08; N, 8.68. Found: C, 77.02; H, 6.627; N, 8.45.

7-(tert-butyl)-5-(4-(tert-butyl)pyridin-2-yl)-2-(2,6-dibenzhydryl-4-methylphenyl)-2,3-dihydroimidazo[1,5-*a*]pyridinium chloride (4e): Following the general procedure of ligand precursors, a product 4e (464 mg, 85% yield) was obtained as white solids from 4,4′-di-tert-butyl-[2,2′-bipyridine]-6-carbaldehyde 2 (500 mg, 0.71 mmol), 2,6-dibenzhydryl-4-methylaniline (312 mg, 0.71 mmol), ethanol (3.5 mL) and chloromethyl ethyl ether (1.33 mL, 14.2 mmol). The cyclization of imine derivative with chloromethyl ethyl ether was completed in 2 days. The crude product was purified through flash column chromatography (CH_2Cl_2:CH_3OH = 10:1). The remaining byproduct was removed by recrystallization with CH_2Cl_2/hexane at a low temperature. ^{1}H NMR (400 MHz, CD_2Cl_2) δ 8.96 (d, *J* = 1.9 Hz, 1H), 8.35 (dd, *J* = 1.9, 0.8 Hz, 1H), 8.13 (dd, *J* = 5.3, 0.7 Hz, 1H), 8.07 (dd, *J* = 1.6, 0.6 Hz, 1H), 7.66 (dd, *J* = 1.8, 0.7 Hz, 1H), 7.43 (d, *J* = 1.7 Hz, 1H), 7.41 (dd, *J* = 5.3, 1.8 Hz, 1H), 7.30–7.17 (m, 6H), 7.09–7.05 (m, 4H), 6.99–6.93 (m, 4H), 6.83 (s, 2H), 6.81–6.72 (m, 6H), 5.14 (s, 2H), 2.25 (s, 3H), 1.45 (s, 9H), 1.44 (s, 9H). ^{13}C NMR (100 MHz, CD_2Cl_2) δ 162.60, 150.07, 148.75, 148.43, 142.40, 141.86, 141.52, 141.49, 132.86, 131.92, 131.49, 130.52, 129.88, 128.90, 128.77, 128.67, 128.34, 127.30, 127.18, 122.30, 120.11, 118.43, 116.06, 114.31, 52.22, 35.57, 35.42, 30.60, 30.07, 21.93. HR-MS (FAB): calcd. for $C_{53}H_{52}N_3$ [M-Cl] 730.4161 found 730.4165. Elemental analysis (%) calcd. for $C_{53}H_{52}ClN_3$: C, 83.05; H, 6.84; N 5.48,. Found: C, 83.01; H, 6.985; N, 5.25.

5-mesityl-2-(pyridin-1-ium-2-ylmethyl)-2H-imidazo[1,5-*a*]pyridinium dichloride (10): The synthetic method for compound **10** is almost analogous to the procedure reported by Aron [97]. Picolinamine (0.18 mL, 1.70 mmol) and paraformaldehyde (80 mg, 2.67 mmol) were stirred in 3.6 mL of ethanol at room temperature for 12 h. Subsequently, 1.25 M HCl in ethanol (2.8 mL, 3.56 mmol) and 6-mesityl-pyridine-2-carboxaldehyde **9** (396 mg, 1.76 mmol) were added and the reaction was maintained at room temperature for 6 h. The solvent was removed by rotary evaporation and the crude mixture was purified using column chromatography (silica, CH_2Cl_2:CH_3OH = 8:1). Recrystallization from CH_3OH/CH_2Cl_2/ether afforded an ivory powder **10** (443 mg, 63% yield). ^{1}H NMR (400 MHz, CD_2Cl_2) δ 9.28 (s, 1H), 8.97 (d, *J* = 1.6 Hz, 1H), 8.43 (d, *J* = 4.8 Hz, 1H), 7.93 (d, *J* = 7.8 Hz, 1H), 7.79 (d, *J* = 9.4 Hz, 1H), 7.68 (td, *J* = 7.7, 1.8 Hz, 1H), 7.29 (dd, *J* = 9.4, 6.8 Hz, 1H), 7.22 (ddd, *J* = 7.6, 4.8, 1.1 Hz, 1H), 7.07 (s, 2H), 6.90 (dd, *J* = 6.8, 1.0 Hz, 1H), 6.25 (s, 2H), 2.34 (s, 3H), 2.00 (s, 6H). ^{13}C NMR (100 MHz, CD_2Cl_2) δ 153.3, 149.7, 141.2, 137.6, 137.5, 134.4, 130.4, 129.5, 127.0, 125.1, 124.9, 124.4, 124.0, 119.3, 117.7, 116.0, 54.8, 21.2, 19.3 HR-MS (FAB): calcd. for $C_{22}H_{22}N_3$ [M-H-2Cl] 328.1814 found 328.1839. Elemental analysis (%) calcd. for $C_{22}H_{23}Cl_2N_3$: C, 66.00; H, 5.79; N, 10.50. Found: C, 66.2; H, 6.239; N, 10.52.

3.4. Synthesis of Ag(I) Complexes. General Procedure

In the absence of light, ligand precursors (1 equiv) and Ag_2O (2 equiv) in CH_2Cl_2 (0.084 M) were stirred in a Schlenk flask at room temperature for 23 h. The crude solution was filtered through a Celite pad with CH_2Cl_2. The volatiles were evaporated in vacuo and washed with distilled hexane (if needed, the crude products were recrystallized using CH_2Cl_2 with hexane).

Synthesis of Ag(I) complex 5: Following the general procedure of Ag (I) complex, a product **5** (292 mg, 84% yield) was obtained as a light-yellow solid from ligand precursor **3** (300 mg, 0.77 mmol), Ag_2O (360 mg, 1.55 mmol), and CH_2Cl_2 (9 mL). X-ray quality crystals were gained by the liquid diffusion of hexane into saturated CH_2Cl_2 at room temperature in the dark. ^{1}H NMR (400 MHz, CD_2Cl_2) δ 8.79 (d, *J* = 4.9 Hz, 1H), 7.92 (td, *J* = 7.7, 1.8 Hz, 1H), 7.71 (d, *J* = 7.8 Hz, 1H), 7.59 (d, *J* = 9.3 Hz, 1H), 7.57–7.46 (m, 3H), 7.31 (d, *J* = 7.8 Hz, 2H), 7.13 (dd, *J* = 9.3, 6.7 Hz, 1H), 6.83 (dd, *J* = 6.7, 1.2 Hz, 1H), 2.24 (sept, *J* = 6.8 Hz, 2H), 1.19 (d, *J* = 6.9 Hz, 6H), 1.13 (d, *J* = 6.9 Hz, 6H). ^{13}C NMR (100 MHz, CD_2Cl_2) δ 152.92, 151.17, 145.77, 138.84, 137.98, 136.36, 132.81, 132.74, 130.85, 125.29, 125.05, 124.43, 123.56, 118.54, 117.17, 114.94, 114.88, 54.38, 54.11, 53.84, 53.57, 53.30, 28.56, 24.57, 24.54. Elemental analysis (%) calcd. for $C_{24}H_{25}AgClN_3$: C, 57.79; H, 5.05; N, 8.42. Found: C, 57.76; H, 5.176; N, 8.40.

Synthesis of Ag(I) complex 6a: Following the general procedure of Ag (I) complex, a product **6a** (352 mg, 96% yield) was obtained as a light-yellow solid from ligand precursor **4a** (300 mg, 0.63 mmol),

Ag_2O (292 mg, 1.26 mmol), and CH_2Cl_2 (7.5 mL). ^1H NMR (400 MHz, CD_2Cl_2) δ 8.66 (dd, *J* = 5.3, 0.7 Hz, 1H), 7.66–7.63 (m, 1H), 7.49–7.41 (m, 2H), 7.39 (d, *J* = 1.9 Hz, 2H), 7.25 (d, *J* = 7.7 Hz, 2H), 6.87 (dd, *J* = 1.9, 0.5 Hz, 1H), 2.33–2.16 (m, 4H), 1.37 (d, *J* = 0.7 Hz, 18H), 1.12 (t, *J* = 7.6 Hz, 6H). ^{13}C NMR (100 MHz, CD_2Cl_2) δ 161.70, 152.87, 150.85, 146.78, 141.09, 138.96, 138.29, 133.10, 133.03, 130.35, 127.04, 122.46, 116.74 (s), 113.80, 113.74, 111.69, 35.26, 35.12, 30.58, 29.98, 24.39, 15.54. Elemental analysis (%) calcd. for $C_{30}H_{37}AgClN_3$: C, 61.81; H, 6.4; N, 7.21. Found: C, 62.19; H, 6.49; N, 7.06.

Synthesis of Ag(I) complex 6b: Following the general procedure of Ag (I) complex, a product **6b** (406 mg, 84% yield) was obtained as a light-yellow solid from ligand precursor **4b** (400 mg, 0.79 mmol), Ag_2O (371 mg, 1.60 mmol) and CH_2Cl_2 (9 mL). ^1H NMR (400 MHz, CD_2Cl_2) δ 8.68 (d, *J* = 5.4 Hz, 1H), 7.68 (d, *J* = 1.9 Hz, 1H), 7.52 (t, *J* = 7.8 Hz, 1H), 7.48 (dd, *J* = 5.4, 1.9 Hz, 1H), 7.40 (d, *J* = 1.6 Hz, 2H), 7.30 (d, *J* = 7.8 Hz, 2H), 6.92 (d, *J* = 2.0 Hz, 1H), 2.26 (sept, *J* = 6.8 Hz, 2H), 1.38 (d, *J* = 6.0 Hz, 18H), 1.18 (d, *J* = 6.9 Hz, 6H), 1.13 (d, *J* = 6.9 Hz, 6H). ^{13}C NMR (100 MHz, CD_2Cl_2) δ 161.46, 152.68, 150.89, 146.99, 145.80, 138.95, 136.45, 133.15, 133.08, 130.78, 124.41, 122.44, 122.43, 116.86, 114.21, 114.15, 111.65, 35.27, 35.15, 30.58, 29.99, 28.60, 24.63, 24.53. Elemental analysis (%) calcd. for $C_{32}H_{41}AgClN_3$: C, 62.90; H, 6.76; N, 6.88. Found: C, 62.98; H, 6.612; N, 6.76.

Synthesis of Ag(I) complex 6c: Following the general procedure of Ag (I) complex, a product **6c** (370 mg, 81% yield) was obtained as a light-yellow solid from ligand precursor **4c** (380 mg, 0.75 mmol), Ag_2O (349 mg, 1.50 mmol), and CH_2Cl_2 (9 mL). ^1H NMR (400 MHz, CD_2Cl_2) δ 8.67 (dd, *J* = 5.3, 0.8 Hz, 1H), 7.66 (dd, *J* = 1.9, 0.8 Hz, 1H), 7.49–7.44 (m, 2H), 7.39 (dd, *J* = 2.9, 1.4 Hz, 2H), 7.30 (dd, *J* = 7.9, 1.4 Hz, 1H), 7.22 (dd, *J* = 7.6, 1.4 Hz, 1H), 6.90 (d, *J* = 1.9 Hz, 1H), 2.31–2.11 (m, 3H), 1.64–1.50 (m, 2H), 1.37 (d, *J* = 4.4 Hz, 18H), 1.18 (d, *J* = 6.9 Hz, 3H), 1.11 (d, *J* = 6.9 Hz, 3H), 0.83 (t, *J* = 7.3 Hz, 3H). ^{13}C NMR (100 MHz, CD_2Cl_2) δ 161.50, 152.74, 150.87, 146.87, 146.04, 139.43, 138.95, 137.53, 133.10, 133.04, 130.38, 127.51, 124.60, 122.43, 116.81, 114.07, 114.00, 111.68, 35.25, 35.14, 33.47, 30.58, 29.99, 28.41, 24.63, 24.56, 24.51, 14.28. Elemental analysis (%) calcd. for $C_{32}H_{41}AgClN_3$: C, 62.9; H, 6.76; N, 6.88. Found: C, 63.22; H, 7.007; N, 6.59.

Synthesis of Ag(I) complex 6d: Following the general procedure of Ag (I) complex, a product **6d** (353 mg, 96% yield) was obtained as a yellow solid from ligand precursor **4e** (300 mg, 0.62 mmol), Ag_2O (287 mg, 1.24 mmol), and CH_2Cl_2 (7 mL). ^1H NMR (400 MHz, CD_2Cl_2) δ 8.66 (d, *J* = 5.3 Hz, 1H), 7.95 (dd, *J* = 13.3, 8.2 Hz, 2H), 7.68 (dd, *J* = 1.9, 0.7 Hz, 1H), 7.53–7.42 (m, 6H), 7.04 (d, *J* = 8.5 Hz, 1H), 6.92 (d, *J* = 1.9 Hz, 1H), 2.23 (s, 3H), 1.40 (s, 9H), 1.37 (s, 9H). ^{13}C NMR (100 MHz, CD_2Cl_2) δ 161.89, 152.98, 150.83, 146.94, 139.03, 135.16, 133.44, 132.78, 130.73,130.12, 128.74, 128.39, 128.06, 126.47, 122.53, 122.37, 122.01, 116.86, 114.00, 111.75, 35.25, 35.15, 30.59, 30.00, 18.20. Elemental analysis (%) calcd. for $C_{31}H_{33}AgClN_3$: C, 63.01; H, 5.63; N, 7.11. Found: C, 63.07; H, 5.685; N, 6.95.

Synthesis of Ag(I) complex 6e: Following the general procedure of Ag (I) complex, a product **6e** (423 mg, 93% yield) was obtained as a yellow solid from ligand precursor **4f** (400 mg, 0.52 mmol), Ag_2O (241 mg, 1.04 mmol), and CH_2Cl_2 (6 mL). ^1H NMR (400 MHz, CD_2Cl_2) δ 8.65 (dd, *J* = 5.3, 0.8 Hz, 1H), 7.56 (dd, *J* = 1.9, 0.7 Hz, 1H), 7.48 (dd, *J* = 5.3, 1.9 Hz, 1H), 7.27–7.11 (m, 12H), 7.01–6.97 (m, 5H), 6.90 (ddd, *J* = 4.7, 2.5, 0.5 Hz, 4H), 6.83 (s, 2H), 6.81 (d, *J* = 1.9 Hz, 1H), 6.33 (d, *J* = 1.7 Hz, 1H), 5.19 (s, 2H), 2.24 (s, 3H), 1.38 (s, 9H), 1.33 (s, 9H). ^{13}C NMR (100 MHz, CD_2Cl_2) δ 161.67, 152.82, 150.79, 146.22, 142.87, 142.71, 141.51, 140.06, 138.74, 138.72, 136.54, 132.21, 132.15, 130.23, 129.70, 129.60, 128.88, 128.72, 126.94, 126.88, 122.27, 116.66, 114.80, 114.74, 111.58, 51.74, 35.27, 35.02, 30.68, 29.98, 21.89. Elemental analysis (%) calcd. for $C_{53}H_{51}AgClN_3$: C,72.89; H,5.89; N,4.81. Found: C,72.96; H,5.774; N, 4.65.

Synthesis of Ag(I) complex 11: Et_3N (2 drops) was added to a Schlenk flask containing activated 4Å molecular sieves (20 mg), ligand 10 (210 mg, 0.64 mmol) and Ag_2O (297 mg, 1.28 mmol, 2.01 equiv) in CH_2Cl_2 (18 mL). The mixture was stirred overnight at room temperature in dark. The crude solution was filtered through a pad of Celite with CH_2Cl_2. To remove Et_3N, purification was carried out by recrystallization from dichloromethane/hexane. The volatiles matters were evaporated in vacuo to give a white solid (240 mg, 80% yield). ^1H NMR (400 MHz, CD_2Cl_2) δ 8.56 (d, *J* = 4.1 Hz, 1H), 7.69–7.62

(m, 2H), 7.43 (d, *J* = 9.3 Hz, 1H), 7.26 (d, *J* = 7.4 Hz, 2H), 7.10 – 6.96 (m, 3H), 6.51 (d, *J* = 6.6 Hz, 1H), 5.59 (s, 2H), 2.40 (s, 3H), 2.02 (s, 6H). ^{13}C NMR (100 MHz, CD_2Cl_2) δ 155.54, 150.02, 141.25, 138.56, 137.61, 136.88, 132.88, 130.31, 129.64, 123.78, 123.48, 122.97, 117.13, 116.01, 112.85, 59.66, 21.59, 19.79. Elemental analysis calcd. (%) for $C_{22}H_{21}AgClN_3$: C 56.13, H 4.50, N 8.93; found: C 55.96, H 4.757, N 8.79.

3.5. Synthesis of Ni(II) Complexes. General Procedure

Ag (I) complexes (1 equiv) were added to a 250 mL Teflon-valve Schlenk flask containing (DME)$NiCl_2$ (1 equiv) in a glove box. The flask was removed from the glove box and dichloromethane was added. The resulting solution was stirred at 60 °C for 8 h. After cooling to room temperature, the solution was filtered through a glass frit containing Celite under argon atmosphere. The solvent was removed under reduced pressure. The crude mixture was transferred to a vial with distilled CH_2Cl_2 and recrystallized from CH_2Cl_2/hexane or washed with hexane. Ni(II) complexes (**7, 8a**–**8e**) do not decompose easily in air without moisture. In a low-humidity environment, they can be quickly filtered using celite under normal atmosphere and the solvent can be removed using a rotary evaporator.

Synthesis of Ni(II) complex 7: Following the general procedure of Ni(II) complexes, a product **7** (188 mg, 95% yield) was obtained as a yellow solid from Ag (I) complex **5** (200 mg, 0.40 mmol), (DME)$NiCl_2$ (89 mg, 0.40 mmol), and CH_2Cl_2 (135 mL). X-ray quality crystals were obtained by the liquid diffusion of hexane into saturated CH_2Cl_2 at room temperature. Elemental analysis (%) calcd. for $C_{24}H_{25}Cl_2N_3Ni$: C, 59.43; H, 5.2; N, 8.66. Found: C, 59.54; H, 5.398; N, 8.27;UV-Vis (CH_2Cl_2): λ(nm) 411; μ_{eff} = 2.99 B.M (at 297K).

Synthesis of Ni(II) complex 8a: Following the general procedure of Ni(II) complexes, a product **8a** (97 mg, 66% yield) was obtained as a red-brown powder from Ag (I) complex **6a** (151 mg, 0.26 mmol), (DME)$NiCl_2$ (57 mg, 0.26 mmol), and CH_2Cl_2 (90 mL). Elemental analysis (%) calcd. for $C_{30}H_{37}Cl_2N_3Ni$: C, 63.3; H, 6.55; N, 7.38. Found: C, 63.18; H, 6.764; N, 7.27; UV-Vis (CH_2Cl_2): λ(nm) 409; μ_{eff} = 2.86 B.M (at 297K).

Synthesis of Ni(II) complex 8b: Following the general procedure of Ni(II) complexes, a product **8b** (170 mg, 89% yield) was obtained as a light-ocher powder from Ag (I) complex **6b** (196 mg, 0.32 mmol), (DME)$NiCl_2$ (71 mg, 0.32 mmol), and CH_2Cl_2 (110 mL). Elemental analysis (%) calcd. for $C_{32}H_{41}Cl_2N_3Ni$: C, 64.35; H, 6.92; N, 7.04. Found: C, 64.2; H, 6.584; N, 6.9; UV-Vis (CH_2Cl_2): λ(nm) 408; μ_{eff} = 3.00 B.M (at 297 K).

Synthesis of Ni(II) complex 8c: Following the general procedure of Ni(II) complexes, a product **8c** (240 mg, 98% yield) was obtained as a light-ocher powder from Ag (I) complex **6c** (250 mg, 0.41 mmol), (DME)$NiCl_2$ (90 mg, 0.41 mmol), and CH_2Cl_2 (140 mL). UV-Vis (CH_2Cl_2): λ(nm) 408. Elemental analysis (%) calcd. for $C_{32}H_{41}Cl_2N_3Ni$: C, 64.35; H, 6.92; N, 7.04. Found: C, 64.16; H, 7.031; N, 6.87; μ_{eff} = 2.56 B.M (at 297 K).

Synthesis of Ni(II) complex 8d: Following the general procedure of Ni(II) complexes, a product **8d** (240 mg, 99% yield) was obtained as a dark-brown powder from Ag (I) complex **6e** (248 mg, 0.42 mmol), (DME)$NiCl_2$ (92 mg, 0.42 mmol), and CH_2Cl_2 (145 mL). UV-Vis (CH_2Cl_2): λ(nm) 407. Elemental analysis (%) calcd. for $C_{31}H_{33}Cl_2N_3Ni$: C, 64.51; H, 5.76; N, 7.28. Found: C, 64.25; H, 5.854; N, 6.91; μ_{eff} = 2.82 B.M (at 297 K).

Synthesis of Ni(II) complex 8e: Following the general procedure of Ni(II) complexes, a product **8e** (290 mg, 99% yield) was obtained as an ocher powder from Ag (I) complex **6f** (300 mg, 0.34 mmol), (DME)$NiCl_2$ (75 mg, 0.34 mmol), and CH_2Cl_2 (117 mL). UV-Vis (CH_2Cl_2): λ(nm) 417. Elemental analysis (%) calcd. for $C_{53}H_{51}Cl_2N_3Ni$: C, 74.06; H, 5.98; N, 4.89. Found: C, 73.72; H, 5.927; N, 4.75; μ_{eff} = 3.09 B.M (at 297 K).

Synthesis of Ni(II) complex 12: Following the general procedure of Ni(II) complexes, a product **12** (172 mg, 90% yield) was obtained as a light-brown powder from Ag (I) complex **11** (198 mg,

0.42 mmol), (DME)$NiCl_2$ (92 mg, 0.42 mmol), and CH_2Cl_2 (140 mL). X-ray quality crystal was obtained by liquid diffusion of *n*-hexane into aturated CH_2Cl_2 at room temperature. UV-Vis (CH_2Cl_2): λ(nm) 490 Elemental analysis (%) calcd. for $C_{22}H_{21}Cl_2N_3Ni$: C, 57.82; H, 4.63; N, 9.19. Found: C, 57.66; H, 4.853; N, 9. μ_{eff} = 3.0 B.M (at 297 K).

3.6. General Procedure for the Synthesis of Lithium Acrylate Using Ethylene and CO_2

Lithium acrylate was synthesized following a modified version of a previously reported procedure.[7b] Inside a glove box, Ni(II) complex (0.05 mmol), LiI (1.25 mmol) and Zn (2.50 mmol) were added into a 4 mL screw-cap vial equipped with a magnetic stir bar. The vial was removed from the glove box and charged with PhCl (2 mL) via a syringe under argon atmosphere. The vial was then stirred for 3 min, and Et_3N (0.35 mL) was injected via a syringe. Under argon atmosphere, the vial was transferred to a 100 mL stainless steel autoclave and was punctured with a flat-cut needle (18 G, 0.6 cm). The autoclave was immediately closed and purged with ethylene gas (10 bar) for 10 min without stirring. The autoclave was pressurized with ethylene (25 bar) and then with CO_2 (5 bar) at room temperature. The autoclave was heated to 60 °C in an oil bath for 12 h. After cooling to room temperature, the pressure was released. D_2O (1 mL) with sodium 3-(trimethylsilyl)-2,2,3,3-d_4-propionate (0.070 mmol), was added to the reaction mixture as an internal standard. After vigorous stirring for 15 min and manual shaking for about 15 min, the D_2O layer was separated from organic phase by centrifugation and filtration. The D_2O layer was washed with ether (2 mL). The amount of acrylate was determined by ^1H NMR of the D_2O layer.

4. Conclusions

In conclusion, a series of new pyridine-chelated ImPy ligand precursors (**3**, **4a**–**4e**, **10**) were prepared, and their catalytic efficiencies for Ni mediated acrylate synthesis from ethylene and CO_2 were investigated. Additionally, py-ImPy^{H}Ni(II)Cl_2 complexes (**3**), py-Im$Py^{t\text{-}Bu}$Ni(II)Cl_2 complexes (**4a**–**4e**) and *N*-picolyl-ImPyNi(II)Cl_2 (**12**) were synthesized from corresponding Ag complexes (**5**, **6a**–**6e**, **11**) through Ag transmetalation protocol and characterized by single-crystal X-ray crystallography. X-ray structures demonstrated that the six-membered chelate rings with a fused pyridine of ImPy were more rigid and planar than those with labile picolyl units at the N atom of ImPy. Ni(II) complexes (**7**, **8a**–**8e**) with strong chelates yielded up to 108% acrylate (TON 1). Catalytic activities of complex **8b** was further improved (TON up to 8.4) by the addition of monodentate phosphine. Currently, we are exploring other NHC ligands in the catalytic acrylate synthesis.

Supplementary Materials: The following are available online at http://www.mdpi.com/2073-4344/10/7/758/s1, Scheme S1: *in-situ* nickel(II) mediated C-H carboxylation of ethylene using CO_2; Scheme S2: Screening of monodentate phosphine additives in acrylate synthesis using ethylene and CO_2; Scheme S3: Screening of bisphosphine ligands in acrylate synthesis using ethylene and CO_2; Scheme S4: Screening of bidentate N-N ligands in acrylate synthesis using ethylene and CO_2; Figure S1: Percent buried volume (%V_{bur}) of Ni(II) complexes; Figure S2–S45: ^1H NMR and $^{13}C\{^1H\}$ NMR spectrum; Figure S46: UV-Vis spectroscopy of **7**, **8a**–**8e**, **12**; Table S2: Crystallographic data and parameters for **3**, **7**, **8b** and **12**.

Author Contributions: Conceptualization, J.K. and S.H.; methodology, J.K. and S.H.; software, J.K. and S.B.; formal analysis, J.K., H.H., S.B., J.L. and S.H.; investigation, J.K., H.H., J.Y.R., S.B., D.-A.P., S.H.L., H.L. and J.L.; data curation, J.K., J.Y.R. and J.L.; writing—original draft preparation, J.K.; writing—review and editing, J.K. and S.H.; visualization, J.K.; supervision, S.H.; project administration, S.H.; funding acquisition, S.H. All authors have read and agreed to the published version of the manuscript.

Funding: This research was supported by the Korea CCS R&D Center (Korea CCS 2020 Project) grant funded by the Korea government (Ministry of Science, ICT & Future Planning) in 2016 (NRF-2014M1A8A1049301).

Conflicts of Interest: The authors declare no competing financial interest.

References

1. Cokoja, M.; Bruckmeier, C.; Rieger, B.; Herrmann, W.A.; Kühn, F.E. Transformation of carbon dioxide with homogeneous transition-metal catalysts: A molecular solution to a global challenge? *Angew. Chem. Int. Ed.* **2011**, *50*, 8510–8537. [CrossRef] [PubMed]
2. Yu, B.; Diao, Z.-F.; Guo, C.-X.; He, L.-N. Carboxylation of olefins/alkynes with CO_2 to industrially relevant acrylic acid derivatives. *J. CO_2 Util.* **2013**, *1*, 60–68. [CrossRef]
3. Kraus, S.; Rieger, B. Ni-Catalyzed Synthesis of Acrylic Acid Derivatives from CO_2 and Ethylene. In *Carbon Dioxide and Organometallics*; Springer: Cham, Switzerland, 2015; pp. 199–223.
4. Limbach, M. Acrylates from alkenes and CO_2, the stuff that dreams are made of. In *Advances in Organometallic Chemistry*; Elsevier: Amsterdam, The Netherlands, 2015; Volume 63, pp. 175–202.
5. Hollering, M.; Dutta, B.; Kühn, F.E. Transition metal mediated coupling of carbon dioxide and ethene to acrylic acid/acrylates. *Coord. Chem. Rev.* **2016**, *309*, 51–67. [CrossRef]
6. Alper, E.; Orhan, O.Y. CO_2 utilization: Developments in conversion processes. *Petroleum* **2017**, *3*, 109–126. [CrossRef]
7. Wang, X.; Wang, H.; Sun, Y. Synthesis of acrylic acid derivatives from CO_2 and ethylene. *Chem* **2017**, *3*, 211–228. [CrossRef]
8. Wu, X.-F.; Zheng, F. Synthesis of Carboxylic Acids and Esters from CO_2. *Top. Curr. Chem.* **2017**, *375*, 4. [CrossRef]
9. Schmitz, M.; Solmi, M.V.; Leitner, W. Catalytic Processes Combining CO_2 and Alkenes into Value-Added Chemicals. In *Organometallics for Green Catalysis*; Springer: Berlin, Germany, 2018; pp. 17–38.
10. Dabral, S.; Schaub, T. The use of carbon dioxide (CO_2) as a building block in organic synthesis from an industrial perspective. *Adv. Synth. Catal.* **2019**, *361*, 223–246. [CrossRef]
11. Solmi, M.V.; Schmitz, M.; Leitner, W. CO_2 as a Building Block for the Catalytic Synthesis of Carboxylic Acids. In *Studies in Surface Science and Catalysis*; Elsevier: Amsterdam, The Netherlands, 2019; Volume 178, pp. 105–124.
12. Weissermel, K.; Arpe, H. Propene Conversion Products. *Ind. Org. Chem.* **2008**, *4*, 267–312.
13. Hoberg, H.; Schaefer, D. Nickel (0)-induzierte C C-verknüpfung zwischen kohlendioxid und ethylen sowie mono-oder di-substituierten alkenen. *J. Organomet. Chem.* **1983**, *251*, c51–c53. [CrossRef]
14. Hoberg, H.; Peres, Y.; Milchereit, A. C–C-Verknüpfung von alkenen mit CO_2 an nickel (O); n-pentesäuren aus ethen. *J. Organomet. Chem.* **1986**, *307*, C41–C43. [CrossRef]
15. Hoberg, H.; Jenni, K.; Angermund, K.; Krüger, C. CC-Linkages of Ethene with CO_2 on an Iron (0) Complex—Synthesis and Crystal Structure Analysis of $[(PEt_3)_2Fe(C_2H_4)_2]$. *Angew. Chem. Int. Ed. Engl.* **1987**, *26*, 153–155. [CrossRef]
16. Hoberg, H.; Peres, Y.; Krüger, C.; Tsay, Y.H. A 1-Oxa-2-nickela-5-cyclopentanone from Ethene and Carbon Dioxide: Preparation, Structure, and Reactivity. *Angew. Chem. Int. Ed. Engl.* **1987**, *26*, 771–773. [CrossRef]
17. Hoberg, H.; Ballesteros, A.; Sigan, A.; Jégat, C.; Bärhausen, D.; Milchereit, A. Ligandgesteuerte Ringkontraktion von Nickela-fünf-in Vierringkomplexe—Neuartige startsysteme für die präparative chemie. *J. Organomet. Chem.* **1991**, *407*, C23–C29. [CrossRef]
18. Alvarez, R.; Carmona, E.; Cole-Hamilton, D.J.; Galindo, A.; Gutierrez-Puebla, E.; Monge, A.; Poveda, M.L.; Ruiz, C. Formation of acrylic acid derivatives from the reaction of carbon dioxide with ethylene complexes of molybdenum and tungsten. *J. Am. Chem. Soc.* **1985**, *107*, 5529–5531. [CrossRef]
19. Alvarez, R.; Carmona, E.; Galindo, A.; Gutierrez, E.; Marin, J.M.; Monge, A.; Poveda, M.L.; Ruiz, C.; Savariault, J.M. Formation of carboxylate complexes from the reactions of carbon dioxide with ethylene complexes of molybdenum and tungsten. X-ray and neutron diffraction studies. *Organometallics* **1989**, *8*, 2430–2439. [CrossRef]
20. Galindo, A.; Pastor, A.; Perez, P.J.; Carmona, E. Bis(ethylene) complexes of molybdenum and tungsten and their reactivity toward carbon dioxide. New examples of acrylate formation by coupling of ethylene and carbon dioxide. *Organometallics* **1993**, *12*, 4443–4451. [CrossRef]
21. Fischer, R.; Langer, J.; Malassa, A.; Walther, D.; Görls, H.; Vaughan, G. A key step in the formation of acrylic acid from CO_2 and ethylene: The transformation of a nickelalactone into a nickel-acrylate complex. *Chem. Commun.* **2006**, *23*, 2510–2512. [CrossRef]

22. Bruckmeier, C.; Lehenmeier, M.W.; Reichardt, R.; Vagin, S.; Rieger, B. Formation of methyl acrylate from CO_2 and ethylene via methylation of nickelalactones. *Organometallics* **2010**, *29*, 2199–2202. [CrossRef]
23. Lee, S.T.; Cokoja, M.; Drees, M.; Li, Y.; Mink, J.; Herrmann, W.A.; Kühn, F.E. Transformation of nickelalactones to methyl acrylate: On the way to a catalytic conversion of carbon dioxide. *ChemSusChem* **2011**, *4*, 1275–1279. [CrossRef]
24. Jin, D.; Schmeier, T.J.; Williard, P.G.; Hazari, N.; Bernskoetter, W.H. Lewis acid induced β-elimination from a nickelalactone: Efforts toward acrylate production from CO_2 and ethylene. *Organometallics* **2013**, *32*, 2152–2159. [CrossRef]
25. Lee, S.T.; Ghani, A.A.; D'Elia, V.; Cokoja, M.; Herrmann, W.A.; Basset, J.-M.; Kühn, F.E. Liberation of methyl acrylate from metallalactone complexes via M–O ring opening (M = Ni, Pd) with methylation agents. *New J. Chem.* **2013**, *37*, 3512–3517. [CrossRef]
26. Plessow, P.N.; Weigel, L.; Lindner, R.; Schäfer, A.; Rominger, F.; Limbach, M.; Hofmann, P. Mechanistic details of the nickel-mediated formation of acrylates from CO_2, ethylene and methyl iodide. *Organometallics* **2013**, *32*, 3327–3338. [CrossRef]
27. Jin, D.; Williard, P.G.; Hazari, N.; Bernskoetter, W.H. Effect of Sodium Cation on Metallacycle β-Hydride Elimination in CO_2–Ethylene Coupling to Acrylates. *Chem. A Eur. J.* **2014**, *20*, 3205–3211. [CrossRef]
28. Pápai, I.; Schubert, G.; Mayer, I.; Besenyei, G.; Aresta, M. Mechanistic details of nickel (0)-assisted oxidative coupling of CO_2 with C_2H_4. *Organometallics* **2004**, *23*, 5252–5259. [CrossRef]
29. Graham, D.C.; Mitchell, C.; Bruce, M.I.; Metha, G.F.; Bowie, J.H.; Buntine, M.A. Production of Acrylic Acid through Nickel-Mediated Coupling of Ethylene and Carbon Dioxide–A DFT Study. *Organometallics* **2007**, *26*, 6784–6792. [CrossRef]
30. Plessow, P.N.; Schäfer, A.; Limbach, M.; Hofmann, P. Acrylate formation from CO_2 and ethylene mediated by nickel complexes: A theoretical study. *Organometallics* **2014**, *33*, 3657–3668. [CrossRef]
31. Li, Y.; Liu, Z.; Cheng, R.; Liu, B. Mechanistic Aspects of Acrylic Acid Formation from CO_2–Ethylene Coupling over Palladium-and Nickel-based Catalysts. *ChemCatChem* **2018**, *10*, 1420–1430. [CrossRef]
32. Hendriksen, C.; Pidko, E.A.; Yang, G.; Schäffner, B.; Vogt, D. Catalytic formation of acrylate from carbon dioxide and ethene. *Chem. A Eur. J.* **2014**, *20*, 12037–12040. [CrossRef]
33. Lejkowski, M.L.; Lindner, R.; Kageyama, T.; Bódizs, G.É.; Plessow, P.N.; Müller, I.B.; Schäfer, A.; Rominger, F.; Hofmann, P.; Futter, C.; et al. The first catalytic synthesis of an acrylate from CO_2 and an alkene—A rational approach. *Chem. A Eur. J.* **2012**, *18*, 14017–14025. [CrossRef]
34. Huguet, N.; Jevtovikj, I.; Gordillo, A.; Lejkowski, M.L.; Lindner, R.; Bru, M.; Khalimon, A.Y.; Rominger, F.; Schunk, S.A.; Hofmann, P.; et al. Nickel-Catalyzed Direct Carboxylation of Olefins with CO_2: One-Pot Synthesis of α, β-Unsaturated Carboxylic Acid Salts. *Chem. A Eur. J.* **2014**, *20*, 16858–16862. [CrossRef]
35. Manzini, S.; Huguet, N.; Trapp, O.; Schaub, T. Palladium-and Nickel-Catalyzed Synthesis of Sodium Acrylate from Ethylene, CO_2, and Phenolate Bases: Optimization of the Catalytic System for a Potential Process. *Eur. J. Org. Chem.* **2015**, *2015*, 7122–7130. [CrossRef]
36. Knopf, I.; Tofan, D.; Beetstra, D.; Al-Nezari, A.; Al-Bahily, K.; Cummins, C.C. A family of cis-macrocyclic diphosphines: Modular, stereoselective synthesis and application in catalytic CO_2/ethylene coupling. *Chem. Sci.* **2017**, *8*, 1463–1468. [CrossRef]
37. Hopkins, M.N.; Shimmei, K.; Uttley, K.B.; Bernskoetter, W.H. Synthesis and Reactivity of 1, 2-Bis(di-iso-propylphosphino)benzene Nickel Complexes: A Study of Catalytic CO_2–Ethylene Coupling. *Organometallics* **2018**, *37*, 3573–3580. [CrossRef]
38. Vavasori, A.; Calgaro, L.; Pietrobon, L.; Ronchin, L. The coupling of carbon dioxide with ethene to produce acrylic acid sodium salt in one pot by using Ni (II) and Pd (II)-phosphine complexes as precatalysts. *Pure Appl. Chem.* **2018**, *90*, 315–326. [CrossRef]
39. Stieber, S.C.E.; Huguet, N.; Kageyama, T.; Jevtovikj, I.; Ariyananda, P.; Gordillo, A.; Schunk, S.A.; Rominger, F.; Hofmann, P.; Limbach, M. Acrylate formation from CO_2 and ethylene: Catalysis with palladium and mechanistic insight. *Chem. Commun.* **2015**, *51*, 10907–10909. [CrossRef] [PubMed]
40. Manzini, S.; Cadu, A.; Schmidt, A.C.; Huguet, N.; Trapp, O.; Paciello, R.; Schaub, T. Enhanced activity and recyclability of palladium complexes in the catalytic synthesis of sodium acrylate from carbon dioxide and ethylene. *ChemCatChem* **2017**, *9*, 2269–2274. [CrossRef]
41. Manzini, S.; Huguet, N.; Trapp, O.; Paciello, R.A.; Schaub, T. Synthesis of acrylates from olefins and CO_2 using sodium alkoxides as bases. *Catal. Today* **2017**, *281*, 379–386. [CrossRef]

42. Knopf, I.; Courtemanche, M.-A.; Cummins, C.C. Cobalt Complexes Supported by cis-Macrocyclic Diphosphines: Synthesis, Reactivity, and Activity toward Coupling Carbon Dioxide and Ethylene. *Organometallics* **2017**, *36*, 4834–4843. [CrossRef]
43. Ito, T.; Takahashi, K.; Iwasawa, N. Reactivity of a Ruthenium (0) Complex Bearing a Tetradentate Phosphine Ligand: Applications to Catalytic Acrylate Salt Synthesis from Ethylene and CO_2. *Organometallics* **2018**, *38*, 205–209. [CrossRef]
44. Rummelt, S.M.; Zhong, H.; Korobkov, I.; Chirik, P.J. Iron-mediated coupling of carbon dioxide and ethylene: Macrocyclic metallalactones enable access to various carboxylates. *J. Am. Chem. Soc.* **2018**, *140*, 11589–11593. [CrossRef]
45. Buchwald, S.L.; Milstein, D. *Ligand Design in Metal Chemistry: Reactivity and Catalysis*; John Wiley & Sons: Hoboken, NJ, USA, 2016.
46. Joannou, M.V.; Bezdek, M.J.; Albahily, K.; Korobkov, I.; Chirik, P.J. Synthesis and Reactivity of Reduced α-Diimine Nickel Complexes Relevant to Acrylic Acid Synthesis. *Organometallics* **2018**, *37*, 3389–3393. [CrossRef]
47. Takahashi, K.; Cho, K.; Iwai, A.; Ito, T.; Iwasawa, N. Development of N-Phosphinomethyl-Substituted NHC-Nickel (0) Complexes as Robust Catalysts for Acrylate Salt Synthesis from Ethylene and CO_2. *Chem. A Eur. J.* **2019**, *25*, 13504–13508. [CrossRef] [PubMed]
48. Seo, H.; Hirsch-Weil, D.; Abboud, K.A.; Hong, S. Development of Biisoquinoline-Based Chiral Diaminocarbene Ligands: Enantioselective S_N2' Allylic Alkylation Catalyzed by Copper−Carbene Complexes. *J. Org. Chem.* **2008**, *73*, 1983–1986. [CrossRef]
49. Snead, D.R.; Seo, H.; Hong, S. Recent developments of chiral diaminocarbene-metal complexes for asymmetric catalysis. *Curr. Org. Chem.* **2008**, *12*, 1370–1387. [CrossRef]
50. Hirsch-Weil, D.; Abboud, K.A.; Hong, S. Isoquinoline-based chiral monodentate *N*-heterocyclic carbenes. *Chem. Commun.* **2010**, *46*, 7525–7527. [CrossRef]
51. Rodig, M.J.; Seo, H.; Hirsch-Weil, D.; Abboud, K.A.; Hong, S. Isoquinoline-based diimine ligands for Cu (II)–Catalyzed enantioselective nitroaldol (Henry) reactions. *Tetrahedron Asymmetry* **2011**, *22*, 1097–1102. [CrossRef]
52. Jaiswal, A.S.; Hirsch-Weil, D.; Proulx, E.R.; Hong, S.; Narayan, S. Anti-tumor activity of novel biisoquinoline derivatives against breast cancers. *Bioorg. Med. Chem. Lett.* **2014**, *24*, 4850–4853. [CrossRef]
53. Park, D.-A.; Ryu, J.Y.; Lee, J.; Hong, S. Bifunctional *N*-heterocyclic carbene ligands for Cu-catalyzed direct C–H carboxylation with CO_2. *RSC Adv.* **2017**, *7*, 52496–52502. [CrossRef]
54. Byun, S.; Seo, H.; Choi, J.-H.; Ryu, J.Y.; Lee, J.; Chung, W.-J.; Hong, S. Fluoro-imidazopyridinylidene Ruthenium Catalysts for Cross Metathesis with Ethylene. *Organometallics* **2019**, *38*, 4121–4132. [CrossRef]
55. Park, D.-A.; Byun, S.; Ryu, J.Y.; Lee, J.; Lee, J.; Hong, S. Abnormal *N*-Heterocyclic Carbene–Palladium Complexes for the Copolymerization of Ethylene and Polar Monomers. *ACS Catal.* **2020**, *10*, 5443–5453. [CrossRef]
56. Diez-Gonzalez, S.; Marion, N.; Nolan, S.P. *N*-heterocyclic carbenes in late transition metal catalysis. *Chem. Rev.* **2009**, *109*, 3612–3676. [CrossRef]
57. Dröge, T.; Glorius, F. The Measure of All Rings—*N*-Heterocyclic Carbenes. *Angew. Chem. Int. Ed.* **2010**, *49*, 6940–6952. [CrossRef] [PubMed]
58. Nelson, D.J.; Nolan, S.P. Quantifying and understanding the electronic properties of *N*-heterocyclic carbenes. *Chem. Soc. Rev.* **2013**, *42*, 6723–6753. [CrossRef] [PubMed]
59. Hopkinson, M.N.; Richter, C.; Schedler, M.; Glorius, F. An overview of *N*-heterocyclic carbenes. *Nature* **2014**, *510*, 485–496. [CrossRef] [PubMed]
60. Prakasham, A.; Ghosh, P. Nickel *N*-heterocyclic carbene complexes and their utility in homogeneous catalysis. *Inorg. Chim. Acta* **2015**, *431*, 61–100. [CrossRef]
61. Danopoulos, A.A.; Simler, T.; Braunstein, P. *N*-heterocyclic carbene complexes of copper, nickel, and cobalt. *Chem. Rev.* **2019**, *119*, 3730–3961. [CrossRef]
62. Nolan, S.P. The development and catalytic uses of *N*-heterocyclic carbene gold complexes. *Acc. Chem. Res.* **2011**, *44*, 91–100. [CrossRef]
63. Froese, R.D.; Lombardi, C.; Pompeo, M.; Rucker, R.P.; Organ, M.G. Designing Pd–*N*-heterocyclic carbene complexes for high reactivity and selectivity for cross-coupling applications. *Acc. Chem. Res.* **2017**, *50*, 2244–2253. [CrossRef]

64. Ogba, O.; Warner, N.; O'Leary, D.; Grubbs, R. Recent advances in ruthenium-based olefin metathesis. *Chem. Soc. Rev.* **2018**, *47*, 4510–4544. [CrossRef]
65. Peris, E.; Crabtree, R.H. Recent homogeneous catalytic applications of chelate and pincer *N*-heterocyclic carbenes. *Coord. Chem. Rev.* **2004**, *248*, 2239–2246. [CrossRef]
66. Normand, A.T.; Cavell, K.J. Donor-Functionalised *N*-Heterocyclic Carbene Complexes of Group 9 and 10 Metals in Catalysis: Trends and Directions. *Eur. J. Inorg. Chem.* **2008**, *2008*, 2781–2800. [CrossRef]
67. Poyatos, M.; Mata, J.A.; Peris, E. Complexes with poly (*N*-heterocyclic carbene) ligands: Structural features and catalytic applications. *Chem. Rev.* **2009**, *109*, 3677–3707. [CrossRef]
68. Biffis, A.; Baron, M.; Tubaro, C. Poly-NHC Complexes of transition metals: Recent applications and new trends. In *Advances in Organometallic Chemistry*; Elsevier: Amsterdam, The Netherlands, 2015; Volume 63, pp. 203–288.
69. Hameury, S.; de Frémont, P.; Braunstein, P. Metal complexes with oxygen-functionalized NHC ligands: Synthesis and applications. *Chem. Soc. Rev.* **2017**, *46*, 632–733. [CrossRef] [PubMed]
70. Gardiner, M.G.; Ho, C.C. Recent advances in bidentate bis(*N*-heterocyclic carbene) transition metal complexes and their applications in metal-mediated reactions. *Coord. Chem. Rev.* **2018**, *375*, 373–388. [CrossRef]
71. Alcarazo, M.; Roseblade, S.J.; Cowley, A.R.; Fernández, R.; Brown, J.M.; Lassaletta, J.M. Imidazo[1,5-*a*]pyridine: A versatile architecture for stable *N*-heterocyclic carbenes. *J. Am. Chem. Soc.* **2005**, *127*, 3290–3291. [CrossRef] [PubMed]
72. Burstein, C.; Lehmann, C.W.; Glorius, F. Imidazo[1,5-*a*]pyridine-3-ylidenes—Pyridine derived *N*-heterocyclic carbene ligands. *Tetrahedron* **2005**, *61*, 6207–6217. [CrossRef]
73. Check, C.T.; Jang, K.P.; Schwamb, C.B.; Wong, A.S.; Wang, M.H.; Scheidt, K.A. Ferrocene-Based Planar Chiral Imidazopyridinium Salts for Catalysis. *Angew. Chem. Int. Ed.* **2015**, *54*, 4264–4268. [CrossRef]
74. Espina, M.; Rivilla, I.; Conde, A.; Díaz-Requejo, M.M.; Pérez, P.J.; Álvarez, E.; Fernández, R.; Lassaletta, J.M. Chiral, Sterically Demanding *N*-Heterocyclic Carbenes Fused into a Heterobiaryl Skeleton: Design, Synthesis, and Structural Analysis. *Organometallics* **2015**, *34*, 1328–1338. [CrossRef]
75. Grande-Carmona, F.; Iglesias-Sigüenza, J.; Álvarez, E.; Díez, E.; Fernández, R.; Lassaletta, J.M. Synthesis and characterization of axially chiral imidazoisoquinolin-2-ylidene silver and gold complexes. *Organometallics* **2015**, *34*, 5073–5080. [CrossRef]
76. Iglesias-Sigüenza, J.; Izquierdo, C.; Díez, E.; Fernández, R.; Lassaletta, J.M. Chirality and catalysis with aromatic N-fused heterobicyclic carbenes. *Dalton Trans.* **2016**, *45*, 10113–10117. [CrossRef]
77. Schwamb, C.B.; Fitzpatrick, K.P.; Brueckner, A.C.; Richardson, H.C.; Cheong, P.H.-Y.; Scheidt, K.A. Enantioselective synthesis of α-amidoboronates catalyzed by planar-Chiral NHC-Cu (I) complexes. *J. Am. Chem. Soc.* **2018**, *140*, 10644–10648. [CrossRef] [PubMed]
78. Chen, W.; Chen, K.; Chen, W.; Liu, M.; Wu, H. Well-Designed *N*-Heterocyclic Carbene Ligands for Palladium-Catalyzed Denitrative C–N Coupling of Nitroarenes with Amines. *ACS Catal.* **2019**, *9*, 8110–8115. [CrossRef]
79. Tang, Y.; Benaissa, I.; Huynh, M.; Vendier, L.; Lugan, N.; Bastin, S.; Belmont, P.; César, V.; Michelet, V. An original L-shape, tunable *N*-Heterocyclic Carbene platform for efficient gold (I) catalysis. *Angew. Chem. Int. Ed.* **2019**, *58*, 7977–7981. [CrossRef]
80. Zhang, J.-Q.; Liu, Y.; Wang, X.-W.; Zhang, L. Synthesis of Chiral Bifunctional NHC Ligands and Survey of Their Utilities in Asymmetric Gold Catalysis. *Organometallics* **2019**, *38*, 3931–3938. [CrossRef]
81. Grohmann, C.; Hashimoto, T.; Fröhlich, R.; Ohki, Y.; Tatsumi, K.; Glorius, F. An iron (II) complex of a diamine-bridged bis-*N*-heterocyclic carbene. *Organometallics* **2012**, *31*, 8047–8050. [CrossRef]
82. Kriechbaum, M.; List, M.; JF Berger, R.; Patzschke, M.; Monkowius, U. Silver and Gold Complexes with a New 1, 10-Phenanthroline Analogue *N*-Heterocyclic Carbene: A Combined Structural, Theoretical, and Photophysical Study. *Chem. A Eur. J.* **2012**, *18*, 5506–5509. [CrossRef]
83. Kriechbaum, M.; Winterleitner, G.; Gerisch, A.; List, M.; Monkowius, U. Synthesis, Characterization and Luminescence of Gold Complexes Bearing an NHC Ligand Based on the Imidazo[1,5-*a*]quinolinol Scaffold. *Eur. J. Inorg. Chem.* **2013**, *2013*, 5567–5575. [CrossRef]
84. Nakano, R.; Nozaki, K. Copolymerization of propylene and polar monomers using Pd/IzQO catalysts. *J. Am. Chem. Soc.* **2015**, *137*, 10934–10937. [CrossRef]
85. Tao, W.J.; Nakano, R.; Ito, S.; Nozaki, K. Copolymerization of ethylene and polar monomers by using Ni/IzQO catalysts. *Angew. Chem. Int. Ed.* **2016**, *55*, 2835–2839. [CrossRef]

86. Tao, W.; Akita, S.; Nakano, R.; Ito, S.; Hoshimoto, Y.; Ogoshi, S.; Nozaki, K. Copolymerisation of ethylene with polar monomers by using palladium catalysts bearing an *N*-heterocyclic carbene–phosphine oxide bidentate ligand. *Chem. Commun.* **2017**, *53*, 2630–2633. [CrossRef]
87. Azouzi, K.; Duhayon, C.; Benaissa, I.; Lugan, N.l.; Canac, Y.; Bastin, S.P.; César, V. Bidentate iminophosphorane-NHC ligand derived from the imidazo[1,5-*a*]pyridin-3-ylidene scaffold. *Organometallics* **2018**, *37*, 4726–4735. [CrossRef]
88. Yasuda, H.; Nakano, R.; Ito, S.; Nozaki, K. Palladium/IzQO-catalyzed coordination–insertion copolymerization of ethylene and 1, 1-disubstituted ethylenes bearing a polar functional group. *J. Am. Chem. Soc.* **2018**, *140*, 1876–1883. [CrossRef]
89. Dong, J.; Li, M.; Wang, B. Synthesis, Structures, and Norbornene Polymerization Behavior of Imidazo[1,5-*a*]pyridine-sulfonate-Ligated Palladacycles. *Organometallics* **2019**, *38*, 3786–3795. [CrossRef]
90. Tao, W.; Wang, X.; Ito, S.; Nozaki, K. Palladium complexes bearing an *N*-heterocyclic carbene–sulfonamide ligand for cooligomerization of ethylene and polar monomers. *J. Polym. Sci. Part A Polym. Chem.* **2019**, *57*, 474–477. [CrossRef]
91. Greenburg, Z.R.; Jin, D.; Williard, P.G.; Bernskoetter, W.H. Nickel promoted functionalization of CO_2 to anhydrides and ketoacids. *Dalton Trans.* **2014**, *43*, 15990–15996. [CrossRef]
92. Gaydou, M.; Moragas, T.; Juliá-Hernández, F.; Martin, R. Site-selective catalytic carboxylation of unsaturated hydrocarbons with CO_2 and water. *J. Am. Chem. Soc.* **2017**, *139*, 12161–12164. [CrossRef] [PubMed]
93. Aresta, M.; Pastore, C.; Giannoccaro, P.; Kovács, G.; Dibenedetto, A.; Pápai, I. Evidence for Spontaneous Release of Acrylates from a Transition-Metal Complex Upon Coupling Ethene or Propene with a Carboxylic Moiety or CO_2. *Chem. A Eur. J.* **2007**, *13*, 9028–9034. [CrossRef] [PubMed]
94. Loch, J.A.; Albrecht, M.; Peris, E.; Mata, J.; Faller, J.W.; Crabtree, R.H. Palladium complexes with tridentate pincer bis-carbene ligands as efficient catalysts for C–C coupling. *Organometallics* **2002**, *21*, 700–706. [CrossRef]
95. Langer, J.; Fischer, R.; Görls, H.; Walther, D. A new set of nickelacyclic carboxylates ("nickelalactones") containing pyridine as supporting ligand: Synthesis, structures and application in C–C–and C–S–linkage reactions. *J. Organomet. Chem.* **2004**, *689*, 2952–2962. [CrossRef]
96. Ebisu, Y.; Kawamura, K.; Hayashi, M. Enantioselective copper-catalyzed 1,4-addition of dialkylzincs to enones using a novel N,N,P-Cu(II) complex. *Tetrahedron Asymmetry* **2012**, *23*, 959–964. [CrossRef]
97. Hutt, J.T.; Aron, Z.D. Efficient, single-step access to imidazo[1,5-*a*]pyridine *N*-heterocyclic carbene precursors. *Org. Lett.* **2011**, *13*, 5256–5259. [CrossRef] [PubMed]
98. Kim, Y.; Kim, Y.; Hur, M.Y.; Lee, E. Efficient synthesis of bulky *N*-Heterocyclic carbene ligands for coinage metal complexes. *J. Organomet. Chem.* **2016**, *820*, 1–7. [CrossRef]
99. De Buysser, K.; Herman, G.; Bruneel, E.; Hoste, S.; Van Driessche, I. Determination of the number of unpaired electrons in metal-complexes. A comparison between the Evans' method and susceptometer results. *Chem. Phys.* **2005**, *315*, 286–292. [CrossRef]
100. Leung, C.H.; Incarvito, C.D.; Crabtree, R.H. Interplay of linker, N-substituent, and counterion effects in the formation and geometrical distortion of *N*-heterocyclic biscarbene complexes of rhodium (I). *Organometallics* **2006**, *25*, 6099–6107. [CrossRef]
101. Hartwig, J. *Organotransition Metal Chemistry: From Bonding to Catalysis*; Univ. Science Books: California, CA, USA, 2010.
102. Ramírez-Monroy, A.; Swager, T.M. Metal chelates based on isoxazoline[60]fullerenes. *Organometallics* **2011**, *30*, 2464–2467. [CrossRef]
103. Wang, C.-Y.; Liu, Y.-H.; Peng, S.-M.; Liu, S.-T. Rhodium (I) complexes containing a bulky pyridinyl *N*-heterocyclic carbene ligand: Preparation and reactivity. *J. Organomet. Chem.* **2006**, *691*, 4012–4020. [CrossRef]
104. Cheng, M.; Moore, D.R.; Reczek, J.J.; Chamberlain, B.M.; Lobkovsky, E.B.; Coates, G.W. Single-site β-diiminate zinc catalysts for the alternating copolymerization of CO_2 and epoxides: Catalyst synthesis and unprecedented polymerization activity. *J. Am. Chem. Soc.* **2001**, *123*, 8738–8749. [CrossRef]
105. Dai, S.; Sui, X.; Chen, C. Highly Robust Palladium (II) α-Diimine Catalysts for Slow-Chain-Walking Polymerization of Ethylene and Copolymerization with Methyl Acrylate. *Angew. Chem. Int. Ed.* **2015**, *54*, 9948–9953. [CrossRef]